STRUCTURAL AND BIOCHEMICAL STUDIES OF BACTERIAL CHEMORECEPTORS

A Dissertation
Presented to the Faculty of the Graduate School
of Cornell University
In Partial Fulfillment of the Requirements for the Degree of
Doctor of Philosophy

by
Abiola Melantha Pollard

February 2010

STRUCTURAL AND BIOCHEMICAL STUDIES OF BACTERIAL CHEMORECEPTORS

Abiola Melantha Pollard, Ph. D.

Cornell University 2010

Transmembrane chemoreceptors, also known as methyl-accepting chemotaxis proteins (MCPs), translate extracellular signals into intracellular responses in the bacterial chemotaxis system. MCPs control the activity of the kinase, CheA, via a coupling protein, CheW. The chemoreceptor, CheA and CheW form a ternary complex that is the central signaling unit in bacterial chemotaxis. Although the individual structures of the components of the ternary complex are known, the precise molecular associations of these proteins has yet to be identified. Here we present a soluble stable ternary complex from *Thermotoga maritima* that can be used to probe the molecular interactions between MCP, CheA and CheW. The stoichiometry of this soluble complex was determined to be one MCP dimer: one CheA dimer: two CheW dimers. In this complex the autophosphorylating activity of CheA was significantly inhibited by the soluble MCP, Tm14. The cytoplasmic portion of a *T. maritima* transmembrane MCP (Tm1143) also inhibited the activity of CheA to varying degrees depending on specific mutations that mimic conditions inside the cell. These results confirm the functional relevance of this ternary complex that will be further rationalized in terms of the structure of the complex. Although an X-ray crystal structure of the ternary complex could not be obtained, the structure of Tm14 was determined. Tm14 is distinct

from previous MCP structures in that Tm14 naturally lacks a transmembrane region.

The 2.15 Å resolution crystal structure of a *T. maritima* soluble receptor (Tm14) reveals distortions in its dimeric four-helix bundle that provide insight into the conformational states available to MCPs for propagating signals. A bulge in one helix generates asymmetry between subunits that displaces the kinase-interacting tip by >25 Å relative to a symmetric model. The maximum bundle distortion maps to the adaptation region of transmembrane MCP's where reversible methylation of acidic residues tunes receptor activity. Minor alterations in coiled-coil packing geometry translates to major structural changes downstream. The Tm14 structure discloses how alterations in local helical structure, which could be induced by changes in methylation state and/or by conformational signals from membrane proximal regions, can reposition a remote domain that interacts with the CheA kinase.

BIOGRAPHICAL SKETCH

I was born on January 17, 1981 in New York City, NY to Bill and Bobbie Pollard. At four years old, I was fortunate enough to gain admittance to Hunter College Elementary School. I then went on to attend Hunter College High School, a competitive public high school in New York City. During the summer after eighth grade I participated in a program called Molecular Biology Enrichment for Youth (MBEY) at Iowa State University. After returning from this summer program, I informed my parents I would become a molecular biologist. However, the following summer after attending Camp Rising Sun (CRS), an international leadership camp, I changed my career goals to international policy maker. I went on to attend college at Yale University with the intention of majoring in Ethics, Politics, and Economics or Political science.

My first semester I enrolled in introductory chemistry, because I needed to fulfill the science requirement of the university, however by the end of the semester I knew I wanted my major to be in the natural sciences. As an undergraduate I received a Mellon Fellowship that allowed me to undertake research in the Berner lab (geochemistry), the Blake lab (biogeochemistry), and the Brudvig lab (bioinorganic chemistry) at Yale. I completed my bachelors of science degree in Chemistry in 2003 and went on to pursue graduate studies in Chemistry and Chemical Biology field at Cornell University. I undertook graduate research under the guidance of Brian Crane and with financial support of the Chemical Biology Initiative Training Grant from the NIH. I received my doctoral degree in August 2009.

To my beloved parents and all my ancestors that came before me whose consistent commitment to education, family, and land, despite hardships, has given me the opportunity to pursue this degree.

ACKNOWLEDGMENTS

I am grateful and thankful to numerous people who have helped me in my learning process while I was pursuing a doctorate degree. I would like to thank my parents for years of love and supporting my education. I like to thank my advisor, Brian Crane, for giving me the opportunity to work in his awesome lab, as well as patience and encouragement when I was in the lab. I would also like to thank Brian for teaching me so much through interesting conservations and through example. I want to thank Alex for her friendship, guidance and support. I would like to thank Sang and Joanne for their training, knowledge and support. I would like to thank Jane for her advice, support and friendship particularly during my first years of graduate school.

I want to thank Anil and Maira Nigam who have really help to shape my graduate experience through their advice, support and understanding. I want to thank Mariya and Sudhamsu, my good friends, for helping me navigate those really difficult times during my graduate career and for being so incredibly understanding. I want to thank Gabriela for support, listening to me and really helping to calm me at times. I want to thank Jaya for commiserating with me, joking around with me and saving me from the guys. I want to thank Bhumit, Mike, Tom, and Anand for years of opposing me, mocking me, and most of all making me laugh. I want to thank Ruchi and Xiaoxiao for inspiring me and being good trainees. I would like to thank Shanette Porter for friendship, support and identifying with me through this experience. I want to thank Kristal Maner for showing me how and encouraging me to have fun. I would like to thank all members of the Crane lab past and present for making graduate school such a good experience. I am

really fortunate to have gotten to know so many amazing people at Cornell University. I want to thank Andy Arvai from Scripps for help with structure determination. I would also like to thank the National Institute of Health for funding my research.

TABLE OF CONTENTS

BIOGRAPHICAL SKETCH iii
DEDICATION iv
ACKNOWLEDGMENTS v
TABLE OF CONTENTS vii
LIST OF FIGURES ix
LIST OF TABLES xi
LIST OF ABBREVIATIONS xii

Chapter 1: Introduction to Bacterial Chemotaxis
1.1 Overview of chemotaxis 1
1.2 CheA: The Kinase of Chemotaxis 4
1.3 Chemoreceptors: Extracellular signal gets translated to the inside the cell . 5
REFERENCES 12
Chapter 2: Stoichiometry and Activity of Ternary Complex
2.1 Introduction 17
2.2 Methods 18
2.2.1 Gene manipulation and Protein expression 18
2.2.2 Pull down assay for binding receptor constructs to kinase 19
2.2.3 Size-exclusion chromatography 19
2.2.4 Radioactive Phosphorylation Assays 20
2.2.5 Analytical Ultracentrifugation: Sedimention equilibrium to measure molecular weight 20
2.2.6 Mass Spectrometry analysis of ternary complex 20
2.3 Results: Binding of Receptor to CheA and CheW 21
2.3.1 Size-exclusion chromatography 21
2.3.2 The stoichiometry of the ternary complex 22
2.3.3 Mass Spectrometry to determine molecular weight of complex 24
2.3.4 Analytical Ultracentrifugation measured the molecular weight of complexes in solution 27
2.3.5 Effect of Receptors on Activity of CheA 29
2.4 Discussion 32
REFERENCES 35
Chapter 3: Structure of Tm14
3.1 Introduction 37
3.2 Materials/Methods: 40
3.2.1 Gene Manipulation 40
3.2.2 Crystallization and Data Collection 41
3.2.3 Structure Determination and Refinement 41
3.2.4 Graphics 41
3.3 Results 42
3.5 Conclusions 64
REFERENCES 67
APPENDIX
A.1 Introduction 75
A.2 Methods 79
REFERENCES 93

LIST OF FIGURES

S.No	Figure ID	Description	Page No.
1	1.1	Simplified Diagram of Bacterial Chemotaxis	3
2	1.2	Model of CheA homodimer with structures of five domains	5
3	1.3	Model of full length chemoreceptor	7
4	2.1	Pull-down with affinity-tagged flTm14 and $Tm14_C$	23
5	2.2	TOF MS spectra of Ternary complex	26
6	2.3	Effect of Cytoplasmic fragments of Receptors on CheA activity	31
7	3.1	Tm14 compared to other known MCP_C structures	44
8	3.2	Structural parameters of the three receptor structures as analyzed by HELANAL	46
9	3.3	Asymmetry between subunits A and B in Tm14	47
10	3.4	Close-up of the bulge distortion	49
11	3.5	Head-to-tail crystal packing interactions of Tm14 within the crystal lattice	52
12	3.6	Relevance of Tar lock-on disulfide bonds to the bulge distortion of Tm14	54
13	3.7	The bulge cause displacement of the Tm14 signaling tip relative to helical stalk	55
14	3.8	Variation in helical packing in different positions throughout the Tm14 structure	57
15	3.9	Illustration of how discontinuities maintain helical register	61
16	3.10	Illustration of how discontinuities aid signaling	62
17	3.11	Hexagonal arrangement of chemoreceptors in the membrane imaged by cryo-EM	65
18	A.1	Four helix bundle structure of extracellular domain of aspartate receptor	76
19	A.2	Full length schematic of chemoreceptor	77
20	A.3	Structure of part of the CACHE domain of CitA	78
21	A.4	Initial Diffraction Pattern of McpB	81

22	A.5	Improved diffraction pattern using sodium malonate as additive	82
23	A.6	Representation of the potential symmetry group for McpB and twinning operation	84
24	A.7	Self-Rotation function of output10.sca [McpB crystal]	87
25	A.8	Self-Rotation function of outSePe2_7.sca [SePe2 – crystal]	88
26	A.9	Self-Rotation function of Se26.sca [SePe26 - crystal]	89
27	A.10	Self-Rotation function of outputx20p21.sca [SePeX2 – crystal]	90
28	A.11	Self-Rotation function of G10output2.sca [G10 crystal cocrystallized with Hg]	91
29	A.12	Self-Rotation function of all_I1I2_6.sca [I1 – crystal – cocrystallized with Hg]	92

LIST OF TABLES

S.No	Table ID	Description	Page No.
1	2.1	Analytical Ultracentrifugation data of T. maritima proteins found in signaling unit	28
2	3.1	Data collection and Refinement Statistics for Tm14	43
3	A.1	Data collected on 5 different crystals	85
4	A.2	A table of some of the data sets collected for McpB	86

LIST OF ABBREVIATIONS

ATP	Adenosine triphosphate
Δ289	P3-P4-P5 domain of CheA
EDTA	Ethylenediaminetetraacetic acid
ESR	Electron Spin Resonance
flTm14	Full length Tm14
MCP	Methyl-accepting Chemotaxis Protein
SAD	Single-wavelength anomalous Diffraction
SAXS	Small Angle X-ray Scattering
SDS	Sodium dodecyl sulfate
Tar	Aspartate receptor
TOF MS	Time of Flight Mass Spectrometry
Tsr	Serine receptor

CHAPTER 1

Introduction to Bacterial Chemotaxis

1.1 Overview of chemotaxis

Bacterial chemotaxis is controlled by a signaling network, which allows bacteria to swim toward attractants (i.e. certain sugars and amino acids) and away from repellents (i.e. heavy metals) (*2*). Underlying chemotaxis is a two-component system, composed of a kinase (CheA) and a response regulator (CheY) that couples the stimulus to the response (Figure 1). In this system the input or stimulus is an extracellular ligand bound which causes an output response to change the direction of the cell. Bacterial cells move using a random walk and alternate between tumbling, where the flagella rotate clockwise and smooth swimming, the flagella rotate counterclockwise (*5*). When there is a spatial gradient of attractant the random walk of the cell is biased such that the straight swimming run that carries the cell up the gradient is extended (*5*).

The fact that bacteria are capable of swimming toward food has been known for more than a century. In 1880, Engelmann discovered bacteria change direction according to an environmental signal (*6*). In the 1970s Julius Adler showed that bacteria are able to sense attractants and repellants with proteins he named chemoreceptors (*7*). Over the past 30 years chemotaxis has become the most well-characterized signal transduction system and has served as a model system for other signal transduction systems.

The most studied chemotaxis system comes from enteric bacteria, mainly *E. coli* and *Salmonella enterica*. Enteric bacteria typically deal with the relatively stable environment of the gut (*2*). It is thought that because of this, enteric species may not require the advanced chemotaxis systems that are

being discovered in other non-enteric bacterial species. The advance in genome sequencing has been instrumental in revealing other types of chemotaxis systems. The diversity of chemotaxis system uncovered has led to the conclusion that *E. coli*, while the best understood, may not be representative of chemotaxis in other species. Supporting this idea is the biochemical and genetic work that has been done on *Bacillus subtilis*. *B. subtilis* has more proteins involved in chemotaxis than *E. coli,* although the input stimulus-output response is the same the effect of the phosphorylated response regulator is reversed (*8*).

Although numerous experiements have elucidated many important features of the chemotaxis system there still remain a significant amount of unanswered questions. Unlike various other signal transduction systems the individual proteins involved in chemotaxis are well characterized in that their function and atomic structures are well known. However, relatively little is known about how the proteins involved in chemotaxis interact on the molecular level. In addition many of the atomic structures of chemotactic proteins come from *Thermotoga maritima* because it is a hyperthermophile and therefore the proteins are more amendable to structural studies. In contrast, the bulk of biochemical work has been done on chemotaxis proteins from other species. Given the variety found in the chemotaxis system, it is important to be able to correlate the structure with the biochemistry work on proteins from the same species. My thesis work has revolved around understanding the biochemistry of some of the structural characterized *T. maritima* proteins as well as important molecular interactions of key chemotaxis proteins in this organism.

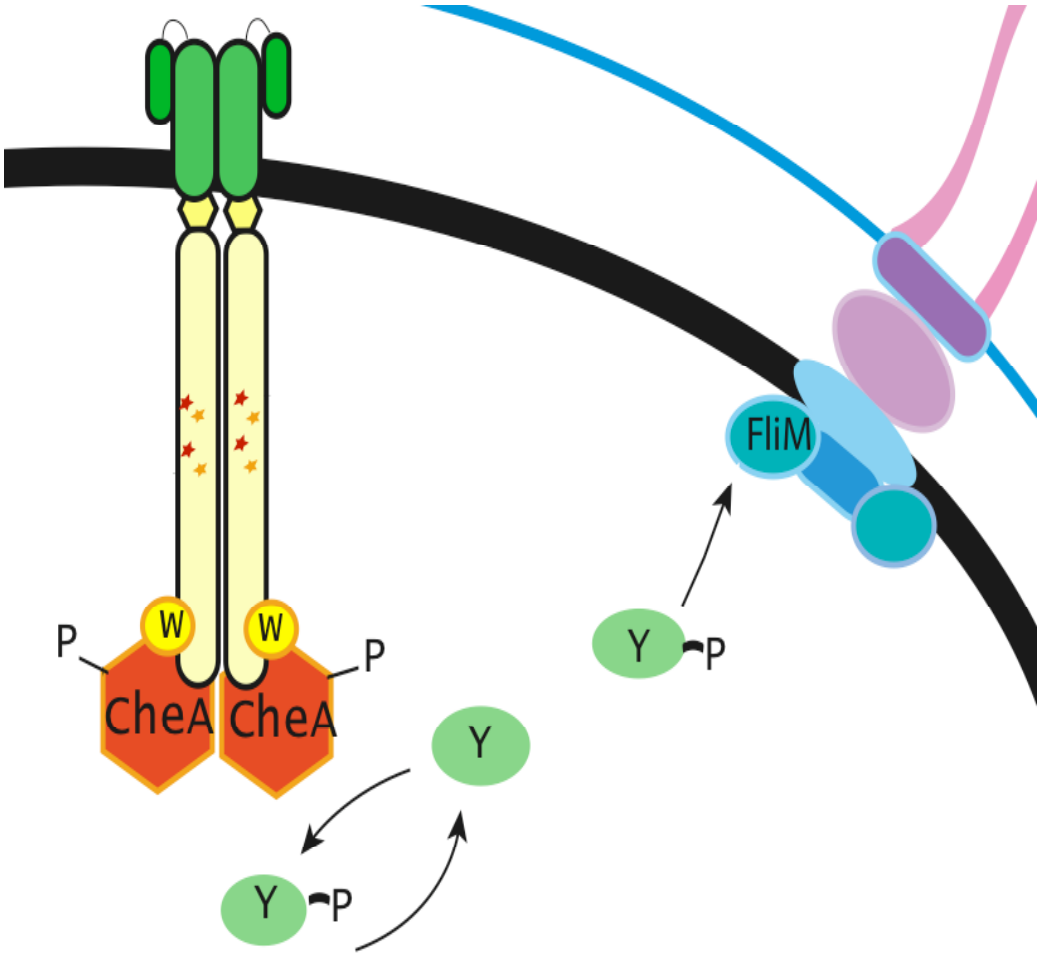

Figure 1.1. Simplified Diagram of Bacterial Chemotaxis –
Two-component system with kinase CheA (red) and response regulator CheY (green). CheY diffuses to the flagellar switch (blue) to determine the direction of flagella (pink) rotation. A chemical compound is sensed by the extracellular domain of the chemoreceptor (green). The activity of CheA is controlled by the chemoreceptor (green and pale yellow) through an adaptor protein CheW (bright yellow). The chemorecptor contains modification sites (stars) that tune the activity of CheA opposite to the effect of the ligand.

1.2 CheA: The Kinase of Chemotaxis

CheA is an autophosphorylating histidine kinase whose activity is central to chemotaxis. CheA consists of five different functional domains. The structures of all five domains have been determined from *T. maritima,* (Figure 1.2)(*9-11*) but the interaction of the different domains is still being worked out. The first domain, called P1, contains the histidine that is phosphorylated (*9*). The phosphate group on the histidine is transferred to an aspartate on CheY the response regulator. CheY docks to the P2 domain of CheA to receive the phosphate from P1. Phospho-CheY interacts directly with the flagellar switch to determine the direction of rotation (*10*). The P3 domain is the dimerization domain, which is required for transautophosphorylation (*12*). The dimers of CheA have been shown to exchange monomers via dissociation of the P3 domain (*13*). The next domain is the P4 domain, also known as the catalytic domain because it contains the ATP binding site (*14*). The P4 domain must interact with P1 domain to transfer the phosphate from ATP to the histidine. The last domain, the P5 domain, binds CheW. The structure of the P5 domain and CheW are similar in that both have the SH3-domain-like fold of two five-stranded β-barrels (*11, 15*). CheW is the protein responsible for coupling the receptor to the CheA kinase. These proteins remain associated in a ternary complex inside the cell and transmembrane sigaling is achieved within this complex (*16*). The phosphorylating activity of CheA has been shown to be affected by the chemoreceptor by as much as 100-fold in the presence of CheW (*17*).

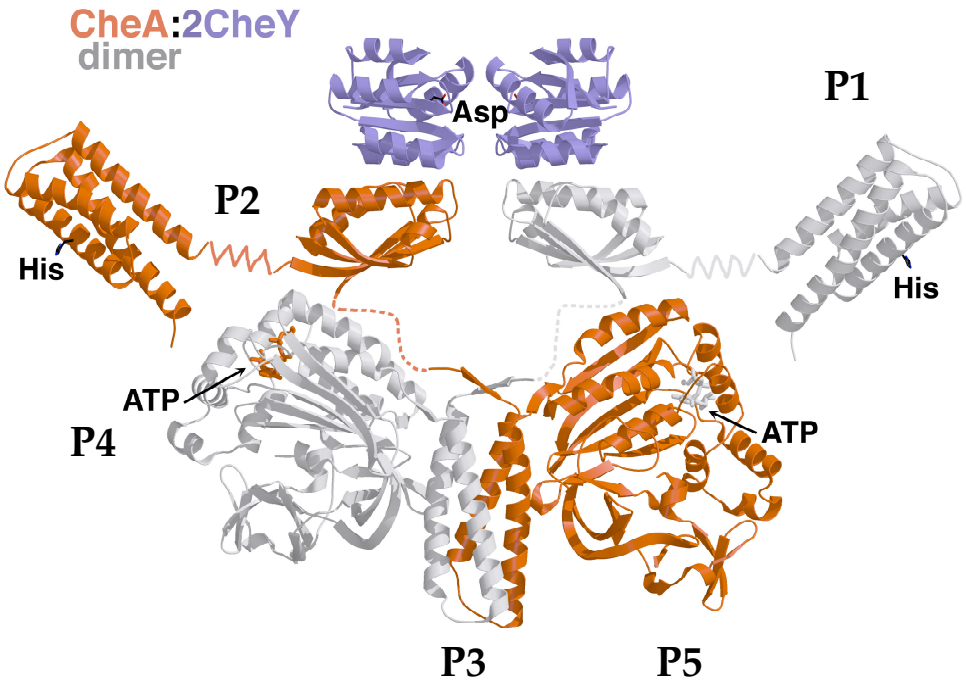

Figure 1.2. Model of CheA homodimer with structures of the five domains. CheY (purple) docks to the P2 domain and thereby facilitates the transfer of a phosphate group from the histidine on P1 to the aspartate on CheY.

1.3 Chemoreceptors: Extracellular signal gets translated to the inside the cell

Chemoreceptors, as known as Methyl-accepting Chemotaxis Proteins (MCPs), are responsible to tuning the activity of the kinase based on extracellular stimuli (Figure 1.3). Chemoreceptors are some of the longest proteins found in the bacterial cell, and are usually about 400 Å from the extracellular domain to the intracellular tip (2). The first step in chemoesensing is for an attractant to bind the extracellular ligand-binding domain of the chemoreceptor. The structure of the ligand-binding domain of the aspartate receptor (Tar) from *E.coli* has been determined to be a pseudo four-helix bundle. It is thought that only one ligand binds one side of the

dimeric extracellular domain at a time (*18*). The method of signal transmission from extracellular domain is unknown. Piston motion of one of the helices has been proposed as the signal through the membrane based on NMR studies, disulfide cross-linking and mutagenesis (*19*). The structure and most of the mechanistic studies on the extracellular domain have been performed on *E. coli* proteins. Secondary structure prediction has found that many chemoreceptors from other species have a PAS-like domain rather than a four-helix bundle. One species with a PAS-like fold as the extracellular domain of the chemoreceptor is *B. subtilis* (*20*). Crosslinking studies of McpB the asparagine receptor of *B. subtilis* indicate that ligand binding might induce a rotation of one of the helices rather than a piston-like motion as modeled for *E.coli* (*21*).

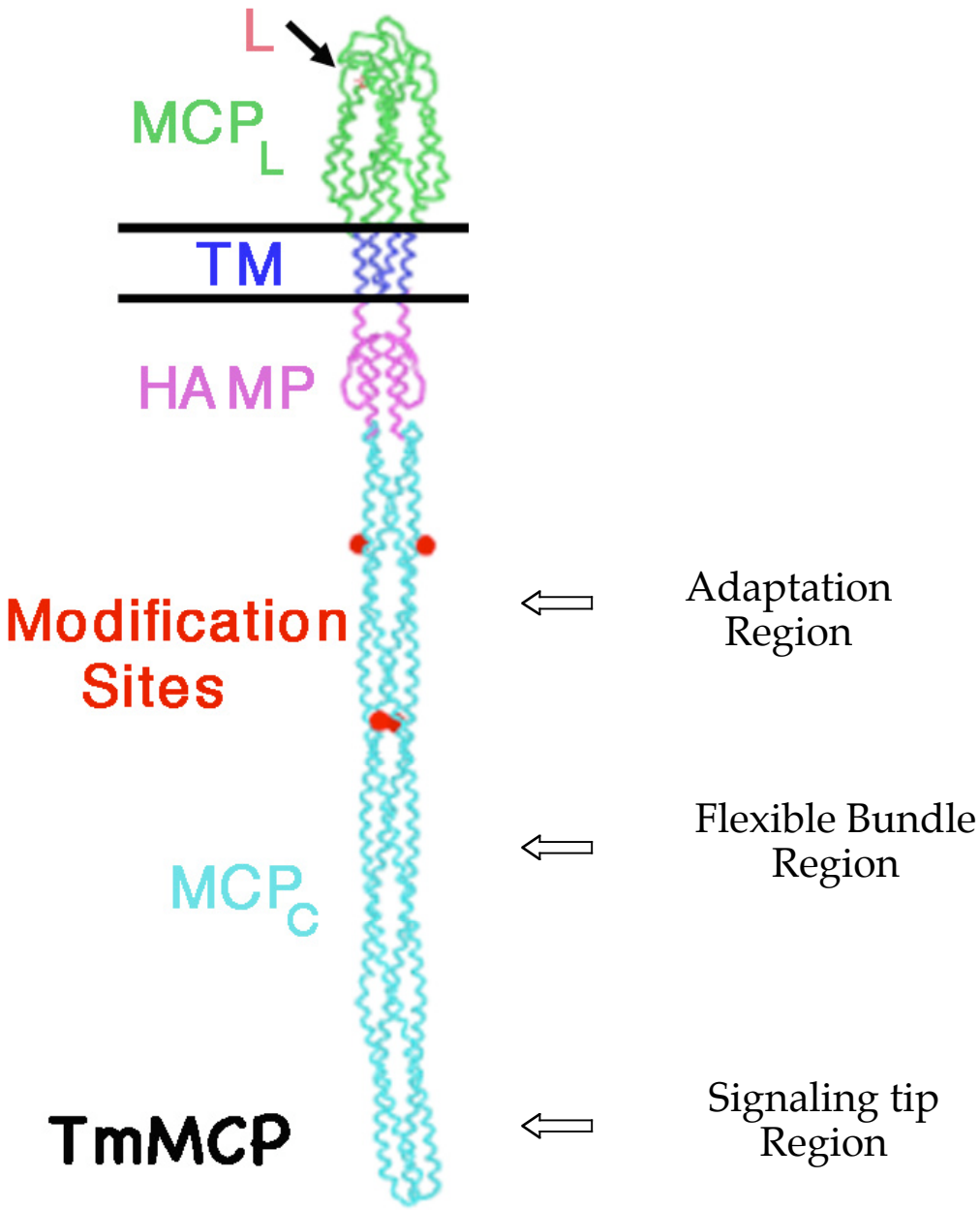

Figure 1.3. Model of full length chemorecptor. Ligand binding domain, MCP_L (green) is from the Tar *E.coli* structure (*1*). The HAMP domain (pink) is a structure from *Archaeoglobus fulgidus* (*3*). The structure of the cytoplasmic domain MCP_C, (blue) is MCP_{1143C} from *T. maritima* (*4*).

After the transmembrane helices of the receptor is the HAMP domain. The HAMP domain is a domain that is commonly present in prokaryotic sensory systems. HAMP domains can be exchanged between two receptors to generate chimeric receptors with altered activity but which is still functional (*22*). Although HAMP domains are a common linker region between extracellular domains and intracellular domains, the exact mechanism by which the signal is transmitted is unknown. A recent NMR structure revealed that the HAMP is a parallel four-helical coiled coil in a different conformation than expected from sequence alone. This different conformation led the authors to propose that the signal is transmitted through the HAMP domain via a rotation of the four helices (*3*). This mechanism is controversial because the structure was of a HAMP domain that naturally lacks a domain downstream, and the rotational model cannot be confirmed with cysteine crosslinking studies on full-length chemoreceptors (*23*).

The next is the cytoplasmic domain, which is the largest domain of the receptor and thus typically broken into three subdomains. The first subdomain is called the adaptation region (*24*). It is called the adaptation region because it contains specific glutamates that become methylated or demethylated by CheR a methyltransferase, and CheB a methylesterase respectively. Some organisms also have CheD, a deamidase, that deamidates certain glutamine residues on the receptor converting them to glutamates. CheD can also act as a methylesterase and CheB can act as a deamidase (*25*). The chemoreceptor in different modification states, with the certain glutamates methylated or demethylated, has a different effect on kinase

activity. These different methylation or demethylation states are mimicked by mutation of the glutamates to glutamine or glutamines to glutamates respectively (*26*). The modification sites affect the activity of the CheA kinase opposite to the affect of the extracellular stimuli thus achieving adaptation and sensitivity. Given that the glutamates that are modified are usually few in number, typically about four, and that the adaptation region is over 140 Å away from where the kinase binds it is fascinating that the modification sites can have such an influence on the activity of the kinase. The mechanism by which methylating or demethylating glutamates change the conformation of the receptor, such that it has a different effect on the kinase activity, is unknown. Whatever the conformational change occurs, presumably it would have to be transmitted through the flexible bundle region of the receptor to the kinase-interacting tip.

The flexible bundle region is a recently characterized subdomain of the cytoplasmic region of the receptor. It is called the flexible bundle region because of staggered packing of the helices leading to a less stable configuration, and key glycine residues that when mutated affect the kinase activity. A wide analysis of chemoreceptors from hundreds of sequenced genomes revealed that the glycines in this region are conserved (*24*). As a result, it is thought that flexibility in this region is very important for signal transduction through the length of the receptor.

The next subdomain is known as the signaling subdomain or protein interacting region because it is the part of the receptor that binds CheA and CheW. This region is the most conserved region of the chemoreceptor (*24*). Many residues in this region are strictly conserved, and therefore thought to be important for interaction with the kinase. It is also thought that residues in

this region are responsible for the chemoreceptor interacting with other chemoreceptors. It has been shown that chemoreceptors cluster with other chemoreceptors inside the cell even with chemoreceptors that bind other ligands (*27*). Studies have shown that by mutating residues in this region, receptor-receptor interactions, as well as the receptor-kinase interaction, can be disrupted (*28*).

The clustering of chemoreceptors is very important to signaling. Immuno-EM experiments have showed that chemoreceptors associate in large clusters at the poles of the cell (*29, 30*). Preclustering receptors using multivalent ligands can increase the sensitivity of the response of the cell to attractant. Thus clustering of receptors help to achieve amplification of the chemical signal (*27*). Recent cryo-EM techniques have been able to visualize the chemoreceptor arrays in wild-type cells (*31, 32*). When the chemoreceptor is overexpressed in *E. coli* hexagonal arrays composed of only chemoreceptors form, demonstrating that chemoreceptors can associate with CheA and CheW inside the cell (*33*). The cryo-EM images reveal a hexagonal arrangement of the chemoreceptors in wild-type cells from several species of bacteria (communication with Adriane Briegel). Within this hexagonal arrangement three receptor dimers can be modeled nicely into the vertices of the hexagonal arrangement. One chemoreceptor has the ability to affect the activity of 36 kinases implying that clustering links a single chemoreceptor to many more kinases (*34*).

Although many different experiments have shown the ability of the chemoreceptor to tune the activity of CheA, the mechanism by which this control is achieved is a big mystery in the field. Molecular details of the CheA-CheW and receptor interactions are still unknown. The stoichiometry

of the Receptor:CheA:CheW complex is also not established as a variety of different stoichiometries have been reported. It is hard to accurately measure stoichiometry and probe molecular interactions in vivo. To understand the ternary complex on a molecular level it is necessary to employ in vitro techniques such as crystallography, dipolar pulsed ESR, small-angle X-ray scattering (SAXS), and activity assays. These techniques are best served by having a soluble, stable, reconstituted system to work on. Because the receptors are transmembrane proteins labs have sought to artificially engineer soluble receptors that still affect the kinase. My thesis work has been to create a soluble ternary complex that could be investigated by a diversity of in vitro techniques, including phosphorylation assays, X-ray crystallography, dipolar pulsed ESR, and SAXS.

REFERENCES

(1) Milburn, M. V., Prive, G. G., Milligan, D. L., Scott, W. G., Yeh, J., Jancarik, J., Koshland, D. E., and Kim, S. H. (1991) 3-Dimensional Structures Of The Ligand-Binding Domain Of The Bacterial Aspartate Receptor With And Without A Ligand. *Science 254*, 1342-1347.

(2) Armitage, J. P. (2006) Bacterial Behavior, in *The Prokaryotes: A Handbook on the Biology of Bacteria* (Dworkin, M., Falkow, S., Rosenberg, E., Schleifer, K., and Stackebrandt, E., Ed.) pp 102-139.

(3) Hulko, M., Berndt, F., Gruber, M., Linder, J. U., Truffault, V., Schultz, A., Martin, J., Schultz, J. E., Lupas, A. N., and Coles, M. (2006) The HAMP domain structure implies helix rotation in transmembrane signaling. *Cell 126*, 929-940.

(4) Park, S. Y., Borbat, P.P., Gonzalez-Bonet, G., Bhatnagar, J., Freed, J.H., Bilwes, A.M., Crane, B.R. (2006) Reconstruction of the chemotaxis receptor:kinase assembly. *Nat. Struct. Mol. Biol. 13*, 400-407.

(5) Segall, J. E., Block, S. M., and Berg, H. C. (1986) Temporal Comparisons In Bacterial Chemotaxis. *Proceedings Of The National Academy Of Sciences Of The United States Of America 83*, 8987-8991.

(6) Drews, G. (2005) Contributions of Theodor Wilhelm Engelmann on phototaxis, chemotaxis, and photosynthesis. *Photosynthesis Research 83*, 25-34.

(7) Adler, J. (1969) Chemoreceptors In Bacteria. *Science 166*, 1588-&.

(8) Szurmant, L., and Ordal, G. W. (2004) Diversity in chemotaxis mechanisms among the bacteria and archaea. *Microbiology And Molecular Biology Reviews 68*, 301-+.

(9) Quezada, C. M., Gradinaru, C., Simon, M. I., Bilwes, A. M., and Crane, B. R. (2004) Helical shifts generate two distinct conformers in the atomic resolution structure of the CheA phosphotransferase domain from Thermotoga maritima. *Journal of Molecular Biology 341*, 1283-1294.

(10) Park, S. Y., Beel, B. D., Simon, M. I., Bilwes, A. M., and Crane, B. R. (2004) In different organisms, the mode of interaction between two signaling proteins is not necessarily conserved. *Proc Natl Acad Sci U S A 101*, 11646-51.

(11) Bilwes, A. M., Alex, L. A., Crane, B. R., and Simon, M. I. (1999) Structure of CheA, a signal-transducing histidine kinase. *Cell 96*, 131-141.

(12) Swanson, R. V., Bourret, R. B., and Simon, M. I. (1993) Intermolecular complementation of the kinase activity of CheA. *Mol. Microbiol. 8*, 435-441.

(13) Park, S. Y., Quezada, C. M., Bilwes, A. M., and Crane, B. R. (2004) Subunit exchange by CheA histidine kinases from the mesophile Escherichia coli and the thermophile thermotoga maritima. *Biochemistry 43*, 2228-2240.

(14) Bilwes, A. M., Quezada, C. M., Croal, L. R., Crane, B. R., and Simon, M. I. (2001) Nucleotide binding by the histidine kinase CheA. *Nature Struct. Biol. 8*, 353-360.

(15) Griswold, I. J., Zhou, H., Matison, M., Swanson, R. V., McIntosh, L. P., Simon, M. I., and Dahlquist, F. W. (2002) The solution structure and interactions of CheW from *Thermotoga maritima. Nature Struct. Biol. in press*.

(16) Gegner, J. A., Graham, D. R., Roth, A. F., and Dahlquist, F. W. (1992) Assembly Of An Mcp Receptor, Chew, And Kinase Chea Complex In The Bacterial Chemotaxis Signal Transduction Pathway. *Cell 70*, 975-982.

(17) Levit, M. N., Liu, Y., and Stock, J. B. (1999) Mechanism of CheA protein kinase activation in receptor signaling complexes. *Biochemistry 38*, 6651-6658.

(18) Falke, J. J., and Hazelbauer, G. L. (2001) Transmembrane signaling in bacterial chemoreceptors. *Trends Biochem. Sci. 26*, 257-265.

(19) Danielson, M. A., Biemann, H. P., Koshland, D. E., and Falke, J. J. (1994) Attractant-Induced And Disulfide-Induced Conformational-Changes In The Ligand-Binding Domain Of The Chemotaxis Aspartate Receptor - A F-19 Nmr-Study. *Biochemistry 33*, 6100-6109.

(20) Anantharaman, V., and Aravind, L. (2000) Cache - a signaling domain common to animal Ca2+ channel subunits and a class of prokaryotic chemotaxis receptors. *Trends In Biochemical Sciences 25*, 535-537.

(21) Szurmant, H., Bunn, M. W., Cho, S. H., and Ordal, G. W. (2004) Ligand-induced conformational changes in the Bacillus subtilis chemoreceptor McpB determined by disulfide crosslinking in vivo. *J Mol Biol 344*, 919-28.

(22) Zhu, Y., and Inouye, M. (2003) Analysis of the role of the EnvZ linker region in signal transduction using a chimeric Tar/EnvZ receptor protein, Tez1. *Journal Of Biological Chemistry 278*, 22812-22819.

(23) Swain, K. E., and Falke, J. J. (2007) Structure of the conserved HAMP domain in an intact, membrane-bound chemoreceptor: A disulfide mapping study. *Biochemistry 46*, 13684-13695.

(24) Alexander, R. P., and Zhulin, I. B. (2007) Evolutionary genomics reveals conserved structural determinants of signaling and adaptation in microbial chemoreceptors. *Proceedings Of The National Academy Of Sciences Of The United States Of America 104*, 2885-2890.

(25) Chao, X., Muff, T. J., Park, S. Y., Zhang, S., Pollard, A. M., Ordal, G. W., Bilwes, A. M., and Crane, B. R. (2006) A receptor-modifying deamidase in complex with a signaling phosphatase reveals reciprocal regulation. *Cell 124*, 561-71.

(26) Hazelbauer, G. L., Falke, J. J., and Parkinson, J. S. (2008) Bacterial chemoreceptors: high-performance signaling in networked arrays. *Trends In Biochemical Sciences 33*, 9-19.

(27) Gestwicki, J. E., and Kiessling, L. L. (2002) Inter-receptor communication through arrays of bacterial chemoreceptors. *Nature 415*, 81-84.

(28) Studdert, C. A., and Parkinson, J. S. (2005) Insights into the organization and dynamics of bacterial chemoreceptor clusters through in vivo crosslinking studies. *Proceedings Of The National Academy Of Sciences Of The United States Of America 102*, 15623-15628.

(29) Maddock, J. R., and Shapiro, L. (1993) Polar location of the chemoreceptor complex in the Escherichia coli cell. *Science 259*, 1717-1723.

(30) Sourjik, V., and Berg, H. C. (2000) Localization of components of the chemotaxis machinery of Escherichia coli using fluorescent protein fusions. *Molecular Microbiology 37*, 740-751.

(31) Briegel, A., Ding, H. J., Li, Z., Werner, J., Gitai, Z., Dias, D. P., Jensen, R. B., and Jensen, G. J. (2008) Location and architecture of the Caulobacter crescentus chemoreceptor array. *Molecular Microbiology 69*, 30-41.

(32) Khursigara, C. M., Wu, X. W., Zhang, P. J., Lefman, J., and Subramaniam, S. (2008) Role of HAMP domains in chemotaxis signaling by bacterial chemoreceptors. *Proceedings Of The National Academy Of Sciences Of The United States Of America 105*, 16555-16560.

(33) Zhang, P. J., Khursigara, C. M., Hartnell, L. M., and Subramaniam, S. (2007) Direct visualization of Escherichia coli chemotaxis receptor arrays using cryo-electron microscopy. *Proceedings Of The National Academy Of Sciences Of The United States Of America 104*, 3777-3781.

(34) Sourjik, V., and Berg, H. C. (2002) Receptor sensitivity in bacterial chemotaxis. *Proc. Natl. Acad. Sci. U S A 99*, 123-127.

CHAPTER 2

THE STOICHIOMETRY AND ACTIVITY OF THE TERNARY COMPLEX

2.1 Introduction

Motile bacteria are capable of temporal sensing across chemical gradients to move to a more favorable chemical environment. The chemotaxis response is controlled by changes in protein phosphorylation in the cytoplasm associated with ligand binding to transmembrane chemoreceptors at the cell surface. This signal transduction system is composed of a set of modular components found in many diverse prokaryotic organisms. The core signaling complex consists of the chemoreceptor, autophosphorylationg histidine kinase CheA and the coupling protein CheW (*1*). We are interested in understanding the interactions of these three components, and how these interactions contribute to signal transduction within the chemotaxis system.

Various techniques and experiments have established that these three components cluster in the cell, and form large complexes of thousands of subunits that are important for signaling (*1-3*). On the molecular level, the composition of the core signaling ternary complex is unknown; although many of the individual chemotaxis proteins have been characterized structurally. The structures of all the domains of CheA are known (*4-6*). In addition there is also a structure of CheAP4P5:CheW complex (*7*). To date there is no structure of a complete transmembrane receptor, but there are structures of the different domains of the receptor, including the cytoplasmic fragment that binds the kinase (*7, 8*). The first structure of the cytoplasmic domain of a chemoreceptor came from the Serine receptor (Tsr) from *E. coli*. The crystal packing of this structure had the dimeric chemoreceptors arranged

as a trimer of dimers (*8*). This structure along with various biochemical studies have led to the model that in *E. coli* there is a trimeric state of chemoreceptors that is critical for signaling (*1*). Another structure of a receptor cytoplasmic domain is MCP_{1143C} from *T. maritima*. The structure of MCP_{1143C} was similar to the Tsr structure in that it was also a long antiparallel four-helix bundle (*7*). However, the crystal packing of MCP_{1143C} was very different; it did not form a trimer of dimers but rather rows of dimers (*7*). The differences in the crystal packing opened up the possibility that the signaling unit found in the two organisms may be different as well.

In addition to the receptor-receptor interaction in the cell, even less is known about how CheA:CheW associates with the cytoplasmic portion of the receptor. The stoichiometry of the ternary complex is an active area of inquiry with different investigators drawing different conclusions. For example, the stoichiometry of the *E. coli* ternary complex Receptor:CheW:CheA has been measured to be 2:2:2, or higher stoichiometries of 24:6:4, and 6.8:3.2:1 (*9-11*). The reason for the discrepancy is uncertain; it could be related to the difference between in vitro versus in vivo measurements. In this work we present the stoichiometry and phosphorylation activity of ternary complex composed of CheA, CheW, and cytoplasmic fragments of receptor from *T. maritima*. This data clearly shows the stoichiometry of the *T. maritima* ternary complex to be 2:2:2, and that the receptor inhibits the activity of the kinase.

2.2 Methods

2.2.1 Gene manipulation and Protein expression

The genes encoding Tm14, Tm1143, CheA (full-length and CheAΔ289), and CheW all from *T. maritima* were PCR cloned into vector pET28a

(Novagen) and expressed with a six-histidine tag in *E. coli* strain BL21(DE3)(Novagen). The cells were growth in Luria broth (U.S. Biological Sciences) with kanamycin (50 μg/mL), and the proteins were purfied using Ni-NTA chelation chromatography as previously described (*4*). The purified protein was run on a Superdex200 26/60 sizing column (GE Healthcare) prior to concentration in 50 mM Tris (pH 7.5) and 150 mM NaCl.

2.2.2 Pull down assay for binding receptor constructs to kinase

The binding of the receptor to CheW and CheAΔ289 was tested via a pull down assay. The receptor constructs contained the six-histidine tag from expression. With CheW and CheAΔ289 the six-histidine tag was cleaved using the thrombin cleavage site built into the histidine tag. The affinity tagged receptor, CheW and CheAΔ289 were incubated for 30 minutes with Ni-NTA resin. After the incubation time the resin was washed four times to remove excess protein that had not bound to the resin or the receptor. The proteins were run on a denatured SDS-PAGE gel to evaluate binding.

2.2.3 Size-exclusion chromatography

The formation of a ternary complex was monitored using molecular sieve size-exclusion chromatography. All purified proteins were run on a Superdex200 26/60 sizing column and the elution profile was monitored at 280 nm. Fractions collected off the column were run on a denaturing SDS-Page gel. All fractions of the ternary complex (receptor, CheAΔ289, and CheW) were run on a denaturing SDS-Page gel. The gel was scanned and the density of the bands of the different protein components of the ternary complex was measured using ImageJ (*12*). The ratio of protein were measured based on density measurements taking the difference in molecular weight into consideration.

2.2.4 Radioactive Phosphorylation Assays

CheA (13 μM) was autophosphorylated by incubation with 0.03 μM [γ-^{32}P] ATP (1.5 μl of 3000 Ci/mmol, 10 μCi/μL, Perkin-Elmer) and 133 μM cold ATP for 2 min in a total volume of 15 μl TKM buffer (50mM Tris [pH 8.5], 50mM KCl, 5mM $MgCl_2$. CheA (13 μM) was pre-incubated for 45 minutes with CheW (20 μM) and Tm14. To quench the CheA autophosphorylation 10 μL of 2X SDS buffer containing 50 mM EDTA was added. The proteins were separated using a 4%-20% Tris-glycine SDS-PAGE gel, and then transferred to an Immuno-Blot PVDF membrane for 30 min at 100 V using transfer buffer (25 mM Tris, 192 mM glycine). The PVDF membrane was exposed to film and the film was developed after 12 hours at –80 C.

2.2.5 Analytical Ultracentrifugation: Sedimention equilibrium to measure molecular weight

Sedimentation equilibrium was performed using the Beckman Coulter analytical ultracentrifuge ProteomeLab XL-1. All samples were run at speeds of 8,000, 12,000, 16,000 and 22,000 rpm to ensure that all components would remain in solution and were not subjected to premature sedimentation. All samples were run for at least 20 hours to allow enough time to reach equilibrium. The initial concentration of the protein samples were 100 μM but this is misleading given that the local concentrations created by the sedimentation could be very different. The sedimentation equilibrium data was analyzed using a program called Ultrascan version 7.2 (*13*).

2.2.6 Mass Spectrometry analysis of ternary complex

The mass spectrometry data to measure the stoichiometry of the ternary complex was collected using Waters Synapt HDMS. The sample was initially analyzed in nanoAcquity LC-TOF MS using Waters' nano-desalting

column under denaturing conditions. Ion mobility separation TOF MS was used to obtain the molecular weight of the ternary complex. TlC chromatogram then LC-MS confirmed that in fact the receptor, CheAΔ289, CheW were all present in the peak corresponding to the ternary complex.

2.3 Results: Binding of Receptor to CheA and CheW

2.3.1 Size-exclusion chromatography

To better study the ternary complex formed by chemoreceptors, CheA and CheW in *T. maritima* we sought soluble fragments of *T. maritima* receptors that could bind CheA:CheW and affect CheA activity. The *T. maritima* genome harbors 7 MCP sequences, 6 of which contain two transmembrane helices and one of which is soluble and annotated as a putative chemoreceptor in the NCBI database (Tm14). The cytoplasmic domains (which comprise the adaptation, flexible, and kinase-interacting regions) of receptors 0429, 1143, 1428, as well as, full-length (fl) Tm14 were cloned into pet28b vectors (Novagen) and expressed with N-terminal His-tags in *E. coli*. (The additional *T. maritima* chemoreceptors were not tested because they are very similar in sequence to the ones cloned and hence expected to have similar binding properties). The purified receptor domains were screened for binding to *T. maritima* CheA and CheW by their ability to pull-down from solution unlabeled, purified, CheW and CheAΔ289 (a stable truncated form of CheA containing domains P3, P4 and P5). In these experiments, Ni-NTA beads were added to solutions of A, W and the target receptors, spun down, washed with high salt (500 mM NaCl) to disfavor non-specific interactions, and run on SDS-PAGE gels. Comparative pull-downs performed with the same protein concentrations under identical conditions found that flTm14 as the receptor

that interacted most strongly with CheAΔ289:CheW (Figure 2.1A). However, as flTm14 was prone to proteolysis, a shorter fragment was generated that removed 40 N- and 24 C-terminal residues to produce a symmetric helical hairpin devoid of overhanging sequences. The shorter fragment, $TM14_C$ (residues 41-254), was much more stable than flTm14, and bound CheAΔ289:CheW with comparable affinity (Figure 2.1A). $Tm14_C$ was further evaluated for its binding stoichiometry with A:W and its ability to affect CheA autophosphoryation.

2.3.2 The stoichiometry of the ternary complex

Protein samples were subject to size-exclusion chromatography to further confirm binding and to initially investigate the stoichiometry of the $Tm14_C$:CheAΔ289:CheW complex. The three proteins were individually purified, and run through a molecular sieve size-exclusion column. There was a clear shift in the elution volume when the receptor was added to CheAΔ289: CheW consistent with the formation of a ternary complex. Because the CheAΔ289:CheW was not saturated by the receptor, the change in elution profile resulted in a bimodal peak, in which the first part of the peak is the ternary complex and latter half is free CheAΔ289:CheW (Figure 2.1B). When we purified the complex by mixing CheAΔ289:CheW with affinity-tagged receptor then using a Ni-NTA column to remove the CheAΔ289:CheW that had not bound the receptor, we were able to obtain a single peak elution profile that consisted of only the ternary complex, $Tm14_C$:CheAΔ289:CheW.

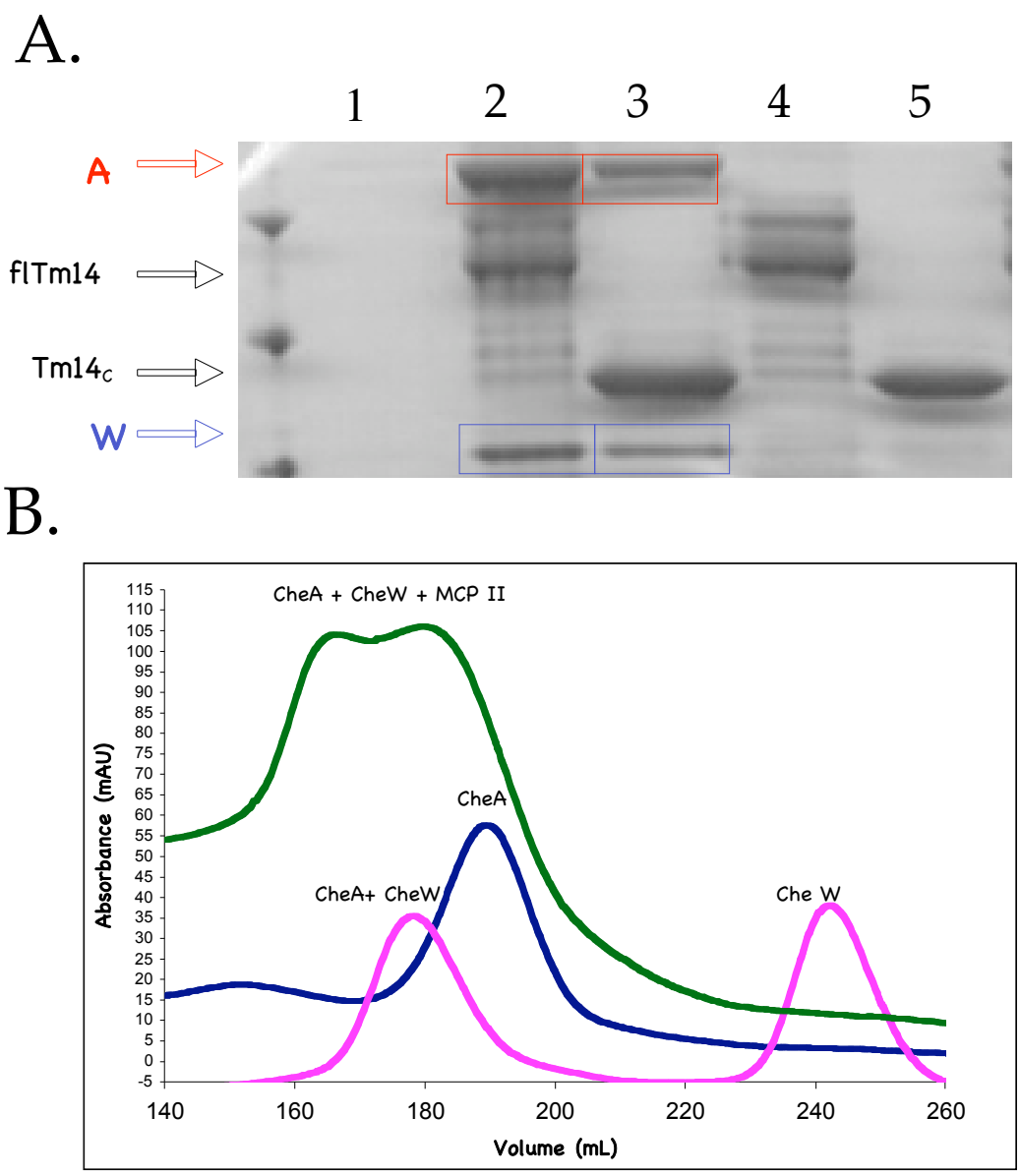

Figure 2.1. Pull-down with affinity-tagged flTm14 and $Tm14_C$
(A.) – Lane 1 – control of untagged CheAΔ289 and CheW with Ni-NTA beads. Lane 2 – flTm14 with his-tag mixed with untagged CheAΔ289 and CheW. Lane 3 – Tm14C with his-tag with untagged CheAΔ289 and CheW. Lane 4 – flTm14 with his-tag. Lane 5 – $Tm14_C$ with his-tag.
Size-Exclusion Chromatography Elution Profiles (B.) – Elution Profiles of CheA alone (blue), CheA + CheW (pink), and CheA + CheW + $Tm14_C$ (green). Peak shift occurs when $Tm14_C$ is added to CheA:CheW.

The different fractions of this ternary complex peak were run on an SDS-Page gel. The densities of the proteins bands on the SDS-Page gel were measured using ImageJ (*12*). By comparing the relative amounts of receptor, CheAΔ289, and CheW we were able to estimate that the elution peak observed contained a low stoichiometry complex of one $Tm14_C$ dimer: CheAΔ289 dimer: two CheW monomers. This complex is termed low stoichiometry because it does not have any higher order associations, other than just the expected dimer of CheA and dimer of receptor. Low stoichiometry is in contrast to the higher stoichiometry complexes that have been measured in *E. coli* such as the trimers of receptor dimer complexes. The expected non-globular shape of the ternary complex prevents accurate determination of molecular weight of the complex from size-exclusion chromatography. However if there were stable higher order complexes consisting of multiple receptor dimers or CheAΔ289 dimers a larger shift in the elution profile then what was observed would be expected. The elution profile and the gel analysis indicated a low stoichiometry complex over a higher order one, however, we have done further experiments to confirm this stoichiometry. For subsequent experiments the ternary complex was purified by size-exclusion chromatography in order to try to maximize the amount of ternary complex in solution.

2.3.3 Mass Spectrometry to determine molecular weight of complex

Ion Mobility Separation TOF Mass spectrometry was able to precisely measure the molecular weight of the ternary complex. Initially it was uncertain as to whether the *T. maritima* ternary complex would dissociate

when converted to the gas phase or during the ionization procedure, which was necessary to accurately measure the mass using this technique. Fortunately, the MS spectra (Figure 2.2) did reveal a peak corresponding to the molecular weight of the low stoichiometry ternary complex, one $Tm14_C$ dimer: one CheAΔ289 dimer: two CheW monomers. The fact that this complex was able to survive the gas phase in significant quantities argues that the complex assembled was not due to non-specific binding. There were three main species found in the mass spectra of the ternary complex. One of the species was CheAΔ289:CheW alone, the second was a CheAΔ289:$Tm14_C$ complex, and the third was the ternary complex. No higher order ternary complexes, consisting of multiple CheA dimers or receptor dimers, were detected by mass spectrometry. All of the three proteins the $Tm14_C$, CheAΔ289, CheW were clearly identified by MS/MS fragmentation thus all three proteins ionized well. Interestingly, the mass spectrometry data was also able to identify a higher order complex consisting of two CheΔ289 dimers: four CheW monomers. Higher order complexes of CheAΔ289 and CheW have been detected using ESR, but are usually only a very small percentage of the CheAΔ289 and CheW in solution (<4%) (Jaya Bhatnagar, unpublished). It was surprising that this 4:4 CheAΔ289:CheW complex could be observed using mass spectrometry but it served to confirm that if there were higher order complexes the technique was sensitive enough that they would likely be detected. Nonetheless, we could not rule out the presence of a minority component of higher order complex that did not survive the gas phase or ionization.

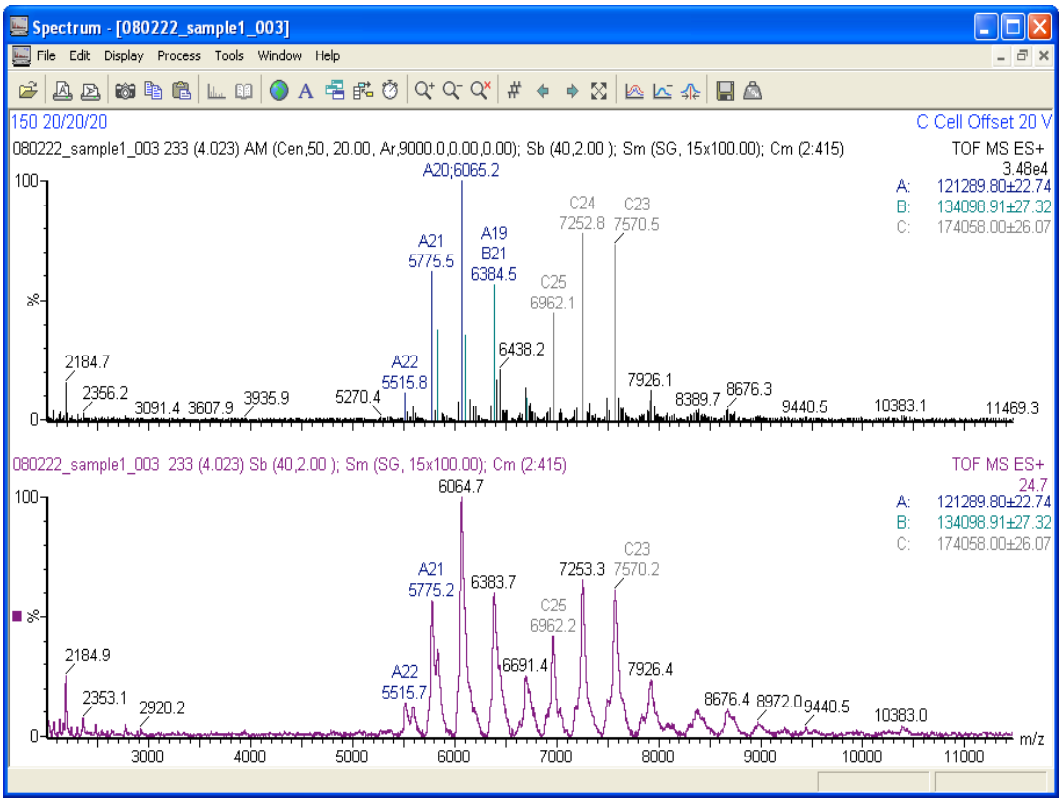

Figure 2.2. TOF MS spectra of Ternary complex. Component A (dark blue) – 121289.80 daltons [CheAΔ289:CheW]. Component B (light blue) – 134098.91 daltons [CheAΔ289:Tm14$_C$]. Component C (gray) – 174058.00 daltons [CheAΔ289:CheW:Tm14$_C$].

2.3.4 Analytical Ultracentrifugation measured the molecular weight of complexes in solution

Analytical ultracentrifugation was used in order to probe the molecular weight of the complex in solution. Specifically sedimentation equilibrium was used because it is a shape-independent technique to measure molecular weight. First the individual components were measured to ensure good agreement with the expected molecular weight (Table 2.1). There are two parameters that are important to examine when determining how good the molecular weight fit the data collected, the number of runs and the variance. The number of runs is a measure of the randomness in the data. If it is too low or too high it means the data deviates in systematic way from the fit. If the deviation of the data from the fit is not random it usually an indication of aggregation and the results are not valid. The number of runs parameter for the data collected was within the reasonable range. The variance is another measure of the quality of the fit to the data, the lower the variance the smaller the difference between the fit and the data, thus the better the fit agrees with the data. All of the samples were investigated at low speed to ensure that larger complexes that might be present were not sedimented too quickly and thus would not be detected. The data collected at low speeds was consistent with the data collected at higher speeds therefore there were no higher molecular weight complexes that had been removed from the solution via quick sedimentation. The data collected on the $Tm14_C$ alone showed no evidence of a higher order organization of the receptor. The sedimentation equilibrium data collected on the ternary complex was also found to be low stoichiometry. The stoichiometry, agreeing well with the mass spectrometry data, was found to be one $Tm14_C$ dimer: CheAΔ289 dimer: two CheW

monomers. It was also confirmed from the sedimentation equilibrium data that there were three species present in solution. One species was the one CheAΔ289 dimer: two CheW monomers, another was one $Tm14_C$ dimer:one CheAΔ289 dimer, and the third being the ternary complex one $Tm14_C$ dimer:one CheΔ289 dimer: two CheW monomers. It is encouraging that the same three species that dominated the mass spectrometry data were again in the sedimentation equilibrium data. Two independent techniques confirmed that there was in fact an absence of higher order complexes of $Tm14_C$:CheAΔ289:CheW. Having established clear binding of CheAΔ289:CheW to a soluble receptor it was important to access whether the receptor was affecting the activity of CheA.

Table 2.1 Analytical Ultracentrifugation data of T. maritima proteins found in signaling unit.

Sample	Model	Fixed Molecular Weights (kD)	Predicted Molecular Weight	Variance	Number of Runs
CheW	One component	17.86	16.95	1.83E-05	37.71%
CheA (P3-P4-P5)	One component	78.87	42.78 (85.56)	3.99E-05	44.08%
Receptor fragment	One component	42.77	24.11(48.22)	2.26E-05	35.15%
CheA (P3-P4-P5) + CheW	Two component	78.34, 117.5	119.46	1.53E-05	33.61%
Receptor fragment CheA(P3-P4-P5) + CheW	Three component	116.9, 146.2, 175.4	119.46, 133.78, 167.68	1.76E-05	34.99%

Parentheses indicate the predicted molecular weight of the dimer. The analyzed data of the ternary complex indicated three species highlighted with a red circle. The first species is a CheAΔ289:CheW complex, the second species $Tm14_C$:CheAΔ289 complex, and the third Tm14C:CheAΔ289:CheW complex

2.3.5 Effect of Receptors on Activity of CheA

To examine the effect on kinase activity on different receptor fragments radioactive phosphorylation assays were employed. In the assay the autophosphorylation of CheA was monitored using the ^{32}P phosphate group that gets transferred to the histidine in CheA. It was found that $Tm14_C$ inhibits CheA autophosphorylation (Figure 2.3A). This inhibitory effect is present even in the absence of CheW and enhanced in the presence of CheW. At concentrations of $Tm14_C$ of 200 μM the activity of the kinase is only 4% of the activity without receptor. The same effect was seen at higher temperature, at 50° C closer to the native environment of the *T. maritima* organism, the effect of the receptor was still inhibitory (the activity of CheA alone was evaluated at 80° C the actual temperature of the *T. maritima* environment but it did not yield consistent results).

Next we wanted to test the effect of receptor modification sites on the activity of CheA. CheR is a methyltransferase that methylates certain glutamates on the receptor. CheD is a deamidase, which deamidates certain glutamines on the receptor. It also has methylesterase activity removing methyl groups placed by CheR (*14*). These modification sites of the receptor have been shown to affect the activity of CheA. According to the consensus sites previously reported (*14*), there are no obvious modification sites found in the full-length Tm14 sequence. Mass spectrometry was unable to clearly identify any methylation sites on Tm14.

Since Tm14 lacked an adaptation region and modification sites, Tm1143 cytoplasmic fragments, which also binds CheA and CheW, were used to test for the effect of modification sites on kinase activity. There was a different

effect on the activity of CheA depending on the modification state of Tm1143. The Tm1143 mutant corresponding to both sites deamidated Q274E Q498E inhibited the kinase significantly more than the unmodified Tm1143 and the Tm1143 (E280Q E504Q) mutant, which mimics the fully methylated state of the receptor (Figure 2.3B). The Tm1143 mutant E280Q only inhibited the kinase by 30% much less than the other constructs of Tm1143 or $Tm14_C$. For the Tm1143 fragments what was important was the position of the modification sites where the receptor was amidated or deamidated not the overall modification state of the receptor. The modification sites are located about 100 Å from the region that interacts with the kinase so it is unlikely that these mutations are having a direct effect on the binding interface with kinase. The fact that different modification states affected the activity of the kinase differently indicates the inhibition observed is probably a specific effect of the receptor binding the kinase.

A.

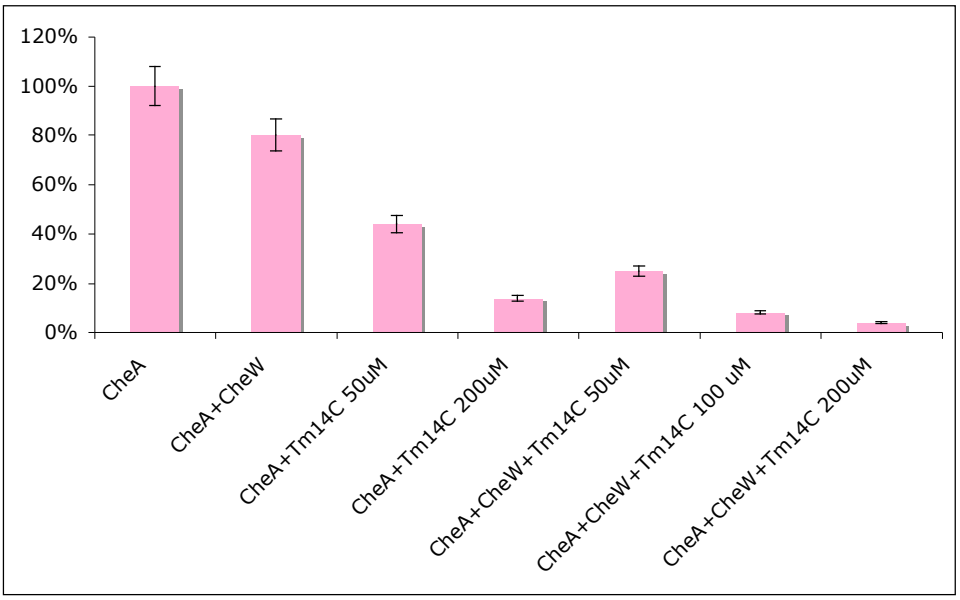

B.

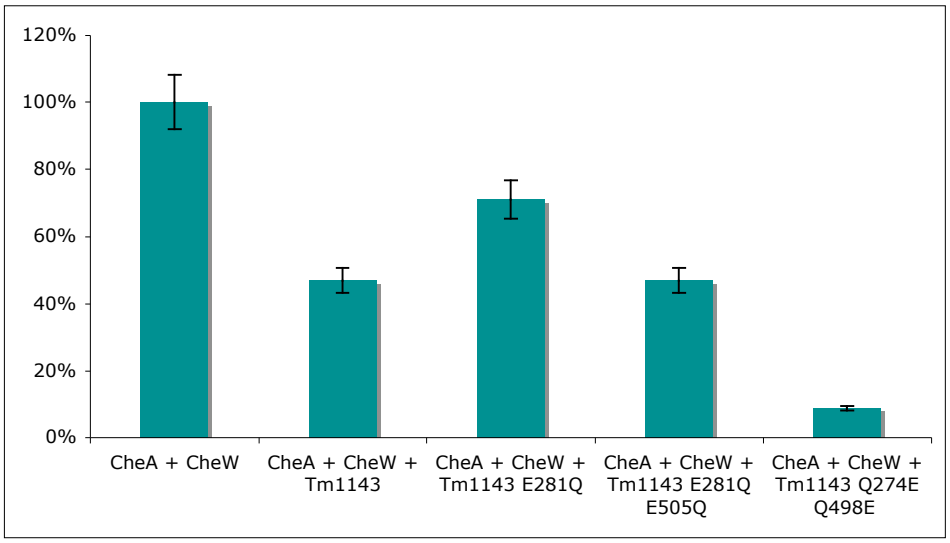

Figure 2.3. Effect of Cytoplasmic fragements of Receptors on CheA activity. Effect of $Tm14_C$ on Normalized CheA activity (A.) Effect of MCP_{1143C} [100 uM] in different modification states on Normalized CheA autophosphorylation activity (B.)

2.4 Discussion

The naturally soluble receptor of *T. maritima* binds CheAΔ289 and CheW to form a soluble ternary complex. Three different techniques were employed to investigate the stoichiometry of the ternary complex, size-exclusion chromatography, mass spectrometry, and sedimentation equilibrium. All three techniques indicate a stoichiometry of one CheAΔ289 dimer: two CheW monomers: one receptor $Tm14_C$ dimer. No higher order ternary complexes or stoichiometry was observed thus it would appear to be very different from the previously characterized *E. coli* soluble complexes. There was no evidence that the receptors of *T. maritima* in vitro form higher order associations as observed in the crystal structure of *E. coli* Tsr (*8*).

This low stoichiometry ternary complex places the kinase in an inhibitory state. The binding of the receptor alone without CheW caused a significant amount of inhibition of the activity of CheA. Also evidence of a CheAΔ289-$Tm14_C$ complex was found in the mass spectrometry data and in the sedimentation equilibrium data. The formation of this complex without CheW is surprising given that the binding of CheAΔ289 for CheW in *T. maritima* is 10 nM (*7*). Although the binding of CheAΔ289 to CheW in *T. maritima* (K_d ~10^{-9}) is stronger than in *E. coli* (K_d ~10^{-5}). The binding of CheAΔ289-CheW to receptor in *T. maritima* (K_d ~10^{-4}) is much weaker than in *E. coli* (K_d ~10^{-6}) (*9*). Although the binding is weak and the stoichiometry of the ternary complex is low (the ratio of the three components is low), the effect of kinase activity argues that the complex was assembled in a relevant way and against non-specific binding. Still it does seem that such weak binding

would not function too well inside the cell, and therefore conceivable that in vivo and in vitro binding constants might be quite different.

Some data, which indicates the in vitro complex is relevant to the in vivo complex, is that activity assays revealed that different modification mutants of MCP_{1143C} receptor fragments had varying effects on the kinase activity. The effect on activity was different depending on which modification sites were present rather than the overall modification state of the receptor as in *E. coli*. The receptors of *T. maritima* belong to the same class of receptors as the *B. subtilis* receptors so it is not surprising that specific modification sites determine the effect on activity as is true for *B. subtilis* (*15*). Additionally *B. subtilis* has a naturally soluble receptor that is similar in length to naturally soluble receptor of *T. maritima*. To date the function of the soluble receptor in *B. subtilis* is unknown, however when a similar receptor is removed from *Borrelia burgdorferi*, via gene deletion, it is completely non-chemotactic (communication with Nyles Charon). Given there is evidence that the cytoplasmic portion of the receptor is the region responsible for clustering a possible function for these smaller soluble receptors is to help cluster transmembrane receptors. Even if it is found that knocking out the soluble receptor in other organisms still renders them chemotactic the soluble receptor could serve as a way of preclustering transmembrane receptors regardless of the extracellular signal. In this way the soluble receptors might enhance the sensitivity of the chemotaxis system because preclustering of receptors has been shown to amplify the chemical signal (2).

Because of the similarities between the *T. maritima* and *B. subtilis* it is expected that attractant would cause an increase in the activity of the kinase in *T. maritima* as well. Thus the receptor inhibiting the kinase would make sense

in order to give the attractant an opportunity to activate the kinase. Another reason for the inhibitory affect of the receptor is the fact the *T. maritima* chemotaxis system must operate at high temperatures. It was seen that the kinase in vitro autophosphorylation rate is faster at higher temperatures closer to the native habitat of *T. maritima*. Perhaps the autophosphrylation rate of *T. maritima* is already so fast that the receptor transmits the signal by inhibiting the basal rate of the kinase by varying degrees. Further experiments are being undertaken to identify conditions under which the *T. maritima* receptors might activate the *T. maritima* kinase. In this work we have characterized a soluble ternary complex, which can further be investigated to find the binding interfaces of the kinase-receptor interaction and to better understand how the receptor is causing the kinase inhibition.

REFERENCES

(1) Hazelbauer, G. L., Falke, J. J., and Parkinson, J. S. (2008) Bacterial chemoreceptors: high-performance signaling in networked arrays. *Trends In Biochemical Sciences 33*, 9-19.

(2) Gestwicki, J. E., and Kiessling, L. L. (2002) Inter-receptor communication through arrays of bacterial chemoreceptors. *Nature 415*, 81-84.

(3) Sourjik, V. (2004) Receptor clustering and signal processing in E. coli chemotaxis. *Trends Microbiol 12*, 569-76.

(4) Bilwes, A. M., Alex, L. A., Crane, B. R., and Simon, M. I. (1999) Structure of CheA, a signal-transducing histidine kinase. *Cell 96*, 131-141.

(5) Quezada, C. M., Gradinaru, C., Simon, M. I., Bilwes, A. M., and Crane, B. R. (2004) Helical shifts generate two distinct conformers in the atomic resolution structure of the CheA phosphotransferase domain from Thermotoga maritima. *Journal of Molecular Biology 341*, 1283-1294.

(6) Park, S. Y., Beel, B. D., Simon, M. I., Bilwes, A. M., and Crane, B. R. (2004) In different organisms, the mode of interaction between two signaling proteins is not necessarily conserved. *Proc Natl Acad Sci U S A 101*, 11646-51.

(7) Park, S. Y., Borbat, P.P., Gonzalez-Bonet, G., Bhatnagar, J., Freed, J.H., Bilwes, A.M., Crane, B.R. (2006) Reconstruction of the chemotaxis receptor:kinase assembly. *Nat. Struct. Mol. Biol. 13*, 400-407.

(8) Kim, K. K., Yokota, H., and Kim, S.H. (1999) Four-helical-bundle structure of the cytoplasmic domain of a serine chemotaxis receptor. *Nature 400*, 787-792.

(9) Gegner, J. A., Graham, D. R., Roth, A. F., and Dahlquist, F. W. (1992) Assembly Of An Mcp Receptor, Chew, And Kinase Chea Complex In The Bacterial Chemotaxis Signal Transduction Pathway. *Cell 70*, 975-982.

(10) Francis, N. R., Wolanin, P. M., Stock, J. B., Derosier, D. J., and Thomas, D. R. (2004) Three-dimensional structure and organization of a receptor/signaling complex. *Proc Natl Acad Sci U S A 101*, 17480-5.

(11) Li, M. S., and Hazelbauer, G. L. (2004) Cellular stoichiometry of the components of the chemotaxis signaling complex. *Journal Of Bacteriology 186*, 3687-3694.

(12) Abramoff, M. D., Magelhaes, P.J., Ram, S.J. (2004) Image Processing with ImageJ. *Biophotonics International 11*, 36-42.

(13) Demeler, B. (2005) UltraScan A Comprehensive Data Analysis Software Package for Analytical Ultracentrifugation Experiments., in *Modern Analytical Ultracentrifugation: Techniques and Methods.* (D. J. Scott, S. E. H. a. A. J. R., Ed.) pp 210-229, Royal Society of Chemistry.

(14) Chao, X., Muff, T. J., Park, S. Y., Zhang, S., Pollard, A. M., Ordal, G. W., Bilwes, A. M., and Crane, B. R. (2006) A receptor-modifying deamidase in complex with a signaling phosphatase reveals reciprocal regulation. *Cell 124*, 561-71.

(15) Szurmant, H., and Ordal, G. W. (2004) Diversity in chemotaxis mechanisms among the bacteria and archaea. *Microbiol Mol Biol Rev 68*, 301-19.

CHAPTER 3

STRUCTURE OF TM14

3.1 Introduction

The bacterial chemotaxis system has served as an important model for understanding transmembrane and intracellular signal transduction (*1-3*). The molecular mechanisms underlying chemotaxis allow bacteria to sense chemical gradients with high sensitivity, wide dynamic range, memory, and signal integration (2). Central to the chemotaxis system is the histidine autokinase, CheA, which phosphorylates CheY, a diffusible regulator of the direction of flagellar rotation (*1-3*). Clusters of transmembrane chemoreceptors, also known as MCPs (for methyl-accepting chemotaxis proteins), engage CheA and through an adaptor protein, CheW, regulate CheA activity in response to ligand binding to the extracellular domain of the receptor (*4-6*). In addition, the MCPs undergo methylation and demethylation of specific glutamate residues in a feedback loop that modifies receptor properties in accordance with the level of kinase activity (*5, 6*). Despite considerable structural and biochemical characterization of MCPs, details are lacking for how the extracellular ligand binding domain affects the membrane-distal cytoplasmic regions where CheA interacts.

MCPs are broadly represented in Bacteria and Archea with multiple paralogs present in a given organism: *E. coli* has four well-studied MCP_S's (Tar, Tsr, Trg and Tap) (*5, 6*), whereas the pathogen *Vibrio cholera* has 45 identifiable MCP sequences (*1*). All biochemically and structurally characterized MCP domains have a dimeric architecture that likely holds for all members due to a universally conserved sequence of repeating

hydrophobic residues that composes the C-terminal dimerization domain. The structural elements of MCPs of the chemoreceptor are as follows: an N-terminal transmembrane helix (TM1) an extracellular ligand-binding domain (which can be variable), a second transmembrane helix (TM2), a cytoplasmic HAMP domain and a C-terminal domain (MCP_C) that folds into a long anti-parallel 4-helix bundle, with two helices supplied from each subunit (Figure 1.3 in Introduction). Crystallographic structures for the *E. coli* Tar and Tsr extracellular domains show a dimer of two antiparallel four helix bundles that bind ligands at their interface (*7*). In contrast, MCP extracellular domains from receptors found in other organisms are expected to have quite different folds (*8*). An NMR structure for a naturally isolated HAMP domain of unknown function reveals an unusual parallel helical bundle structure, with two helices supplied from each subunit (*9*). Recent biochemical and genetic data strongly suggests that this structure is relevant for the HAMP domains within the *E. coli* MCPs (*10, 11*).

Structural changes in the extracellular and HAMP domain translate into conformational changes in the cytoplasmic domain (MCP_C) that affect the activity of CheA. MCP_C can be further broken down into functional subdomains. Most proximal to the membrane is the adaptation region, which contains glutamine and glutamate residues that undergo covalent modification (*6*). Methylation of the Glu (and deamidation of Gln residues in certain receptors) affects ligand binding and CheA activation (*12-15*). The region with the highest sequence conservation is the membrane distal tip of the receptor that binds CheA and CheW. The subdomain between the adaptation region and signaling region has been defined as the flexible bundle region because it contains Gly residues important for function, higher thermal

(B) -factors in crystal structures, and less canonical coiled-coil packing (*8*). There are considerable data for how conformational signals propagate from the ligand binding site, through TM2 to the HAMP domain for the *E. coli* MCPs Tar, Tsr, and Trg. Crosslinking studies, solid-state NMR, spin-label measurements, and replacement of membrane interfacial residues all indicate a piston-like motion of TM2 when ligands bind the extracellular domains (*16-20*) (*5, 6*). Less is known about how these signals affect MCP_C and CheA. Furthermore, the length of MCP_C can vary greatly among receptors, which can be classified based on the number of heptad repeats present in the 4-helical coiled-coil (28-44)(*8*). Crystal structures have been determined for a truncated form of MCP_C from *E. coli* Tsr (class 36) (*21, 22*) and MCP_C 1143 from *T. maritima* ($Tm1143_C$ class 44) (*23*). Both structures depict similar 4-helix bundles, although the C-terminal ends of Tsr_C are frayed due to truncation of the N-terminal helices (*21*). Tsr_C and $Tm1143_C$ also form very different packing interactions within their respective crystal lattices: Tsr_C forming a trimer of dimers (*21*), and $Tm1143_C$ an aligned hedgerow of dimers (*23*). There is strong evidence in *E. coli* that the MCPs do form trimers in the higher order structures that constitute the receptor arrays (*4, 6, 24*), although little is known about how the trimers associate with each other, CheA, and CheW. Whole cell tomography in several bacteria has revealed a hexagonal lattice for the arrays, which is fit well by a trimer-of-dimers (*24-26*). Nonetheless, $Tm1143_C$ does not form a trimeric structure in the crystal, although contacts between the molecules may be influenced by the low pH at which the crystals were grown (*23*). Direct contacts between neighboring molecules in the lattice are mediated by protonated Glu residues. Additional structures, crystallized under different conditions would be helpful to better explore the

conformational states and detailed interactions possible among MCP_C domains.

In addition to the transmembrane MCPs, there are related proteins in many bacteria that have an MCP_C domain, but no transmembrane regions and are hence predicted to be soluble receptors (MCP_S). As result it is unclear what ligands if any these soluble receptors might bind yet they all contain the strictly conserved residues of the transmembrane chemoreceptor and presumbly interact with the kinase. MCP_Ss have CheA-interacting regions and N-terminal or C-terminal extentions beyond the four-helix bundle that can be as small as a positively charged peptide, or as large as an entire domain(s) (e.g. *P. aeruginosa* McpS or *R. sphaeroides* TlpC) (*27, 28*). Herein, we report the structure of MCP_S from *T. maritima* (Tm14). Tm14 has a small positively charged N-termianl peptide that extents beyond the bundle and no known modification sites. Tm14 does have sequence and overall structure similarity to $Tm1143_C$; however its conformation is strikingly different in ways that provide insight into the conformational states available to cytoplasmic domains of chemoreceptors.

3.2 Materials/Methods:

3.2.1 Gene Manipulation

The gene encoding Tm14 was PCR cloned into vector pET28a (Novagen) and expressed with a 6-Histidine tag in *E. coli* strain BL21 (RIL DE3) (Novagen). The cells were grown in Luria Broth (US Biological Sciences) with kanamycin (50 μg/mL) and the proteins were purified using Ni-NTA chelation chromatography as previously described (*29*). The purified protein was run on a Superdex200 26/60 sizing column prior to concentration (15 mg/mL) in 50 mM Tris, pH 7.5/150 mM NaCl. The Asn217Ile mutant was

constructed with Quickchange mutagensis (Novagen) and expressed as described above.

3.2.2 Crystallization and Data Collection

Crystals of Tm14 fragment grew by vapor diffusion against a reservoir of 25% Dioxane after 4 days at room temperature. Pb derivatives were produced by soaking the crystal with 8.7 mM lead trimethyl acetate for 1 hour. Native diffraction data were collected under a 100 K nitrogen stream using a rotating anode X-ray generator with an R-AXIS IV detector (Rigaku). Anomalous diffraction data were collected at 13.1 KeV on the Pb derivative under a 100 K nitrogen stream at the Cornell High Energy Synchrotron Source beamline (F2) on an ADSC Quantum 315 CCD. In both cases 20% ethylene glycol was used as a cryoprotectant. The crystals belong to the space group $P2_1$ and contain one Tm14 dimer per asymmetric unit. Data were processed by HLK2000 (*30*) and XDS (*31*).

3.2.3 Structure Determination and Refinement

Diffraction data from both the native and Pb-derivatized crystals were processed with SOLVE and RESOLVE(*32-34*) to generate initial electron density maps based on anomalous diffraction from Pb and isomorphous differences between the Pb and native data (figure-of-merit = 0.4 to 2.6 Å resolution). A partial structure was built into the initial maps and then helices from the model were used as probes for molecular replacement with PHASER (*35*) to place the missing helical regions. Positional and thermal parameters were refined with CNS amidst cycles of manual model building and solvent molecule placement (*36*).

3.2.4 Graphics

Molecular representations were made with Molscript (*37*) and SPOCK (*37*). Solvent accessible (molecular) surfaces calculated with SPOCK (*37*) using a solvent probe of radius 1.4 Å.

3.3 Results

Tm14 (278 residues, MW = 31,660 kD, and pI = 5.23) has a positively charged 15 residue peptide that extends beyond the predicted 4-helix bundle. When expressed recombinantly in *E. coli*, the purified protein inhibits the autophosphorylation activity of *T. maritima* CheA in a manner that is augmented by the presence of CheW (data shown in previous chapter). The full-length protein had a tendency to degrade over time and thus a more stable, symmetric variant (residues 41-254) was produced for crystallization.

Crystals of the truncated Tm14 (space group P21, a = 68.71 b = 25.75 c = 119.61 β = 93.81) grew in 20% dioxane and diffracted to 2.15 Å resolution, which far exceeds that of the other two known MCP_C structures (PDB codes 1QU7 and 2CH7). The Tm14 structure was determined by single wavelength anomalous diffraction (SAD) of Pb-soaked crystals and refined to R = .254 and R_{free} = .280 (Table 3.1).

Similar to $Tm1143_C$ and Tsr_C, the structure of Tm14 forms a dimeric antiparallel four-helix bundle (Figure 3.1), with each helix having a heptad repeat of hydrophobicity that is commonly found in coiled-coils (i.e. *a-b-c-d-e-f-g* with the *a* and *d* residues mostly hydrophobic and buried inside the core of the dimer interface). However, unlike the structures of $Tm1143_C$ and Tsr_C, Tm14 has an unusual distortion in its middle and shows deviations from the standard helical packing patterns (Figures 3.3 and 3.4). This "bulge" separates the helices and allows a water molecule to penetrate the hydrophobic core. The bulge, which resides at a position analogous to that of MCP modification

Table 3.1. Data collection and Refinement Statistics for Tm14

Diffraction Statistics			
Space group = $P2_1$ (β = 93.81)	a = 68.71	b = 25.75	c = 119.61
	Native Tm14	Pb Tm14	Tm14 Asn217Ile
Resolution (Å)	2.16 (2.22 – 2.16)[g]	2.15 (2.21 – 2.15)[g]	3.00 (3.11 – 3.00)
Number of unique reflections	24221	45726	8972
Number of observations	70197	168739	31676
% Completeness	96.5	97.5	99.8
I/σI [a]	12.3 (4.6)[g]	16.9 (6.1)[g]	22.5 (6.3)
R_{Sym} [b] (%)	6.1 (23.6)[g]	6.2 (20.3)[g]	16.4 (47.6)

SAD structure solution statistics	
Resolution cut-off (Å)	2.50
Number of Anomalous sites found	2
Mean figure of merit	0.38
Overall Z-score	6.59

Refinement Statistics	Native Tm14	Asn217Ile
Number of residues	426	426
Resolution	2.17 (50 – 2.17)	3.00 (20.0 – 3.00)
Wilson B	39.3	52.6
Number of water molecules	424	416
R[c] (%)	24.2(38.5)[g]	25.9 (26.4)
R_{free} [d] (%)	27.8 (41.4)[g]	30.5 (32.8)
Overall B [e] (Å^2)	45.6	58.1
Mainchain B (Å^2)	40.8	52.5
Sidechain B (Å^2)	46.0	59.3

[a] Intensity of the signal to noise ratio. [b] $R_{Sym} = \Sigma\Sigma_j|I_j - \langle I \rangle|/\Sigma\Sigma_j I_j$. [c] $R = \Sigma||F_{obs}|-|F_{calc}||/\Sigma|F_{obs}|$ for all reflections (no σ cutoff). [d] R_{free} calculated against 10% of reflections removed at random. [e] Overall model average thermal B factor. [f] Root mean square deviations from bond and angle restraints. [g] Highest resolution bin for compiling statistics.

sites in the adaptational regions, affects the overall shape of the helix bundle (Figures 3.4 and 3.6).

There are two general packing arrangements found in anti-parallel 4-helix coiled-coils. In one class, the relative offset of the heptad repeats on N- and C-terminal helices is half of one heptad, which would place the 4 interior

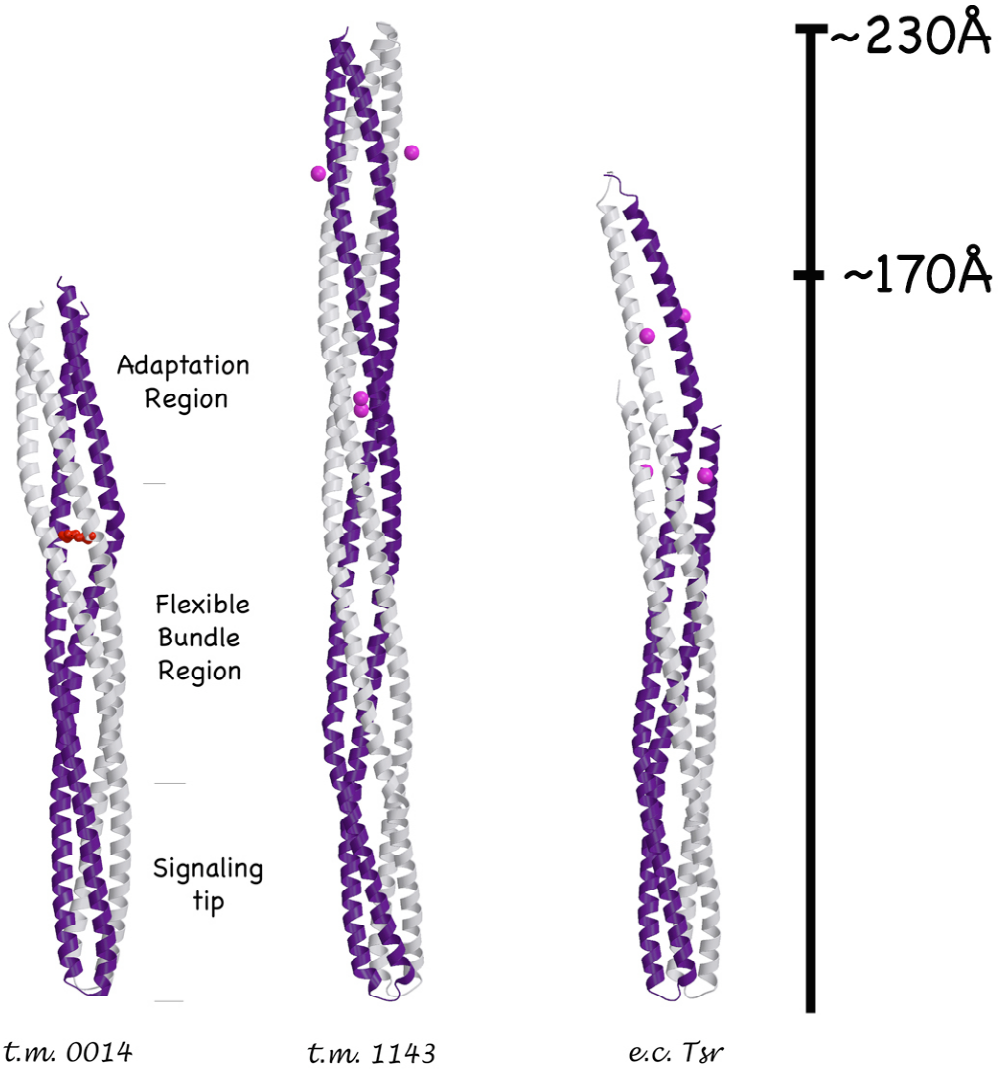

Figure 3.1. Tm14 compared to other known MCP_C structures. Chain A (gray) and Chain B (purple). Methylation sites on $Tm1143_C$ and *E. coli* Tsr_C (magenta spheres) are found in the same region as the Tm14 bulge (red).

residues in roughly the same plane perpendicular to the supercoil axis. However, Tm14 and the other chemoreceptors have an offset of 0.25/heptad, which interdigitates the hydrophobic sites on N- and C-terminal helices. This smaller offset is typical of a ferritin-like coiled-coil such as the Lac repressor

((*38*) and PDB code: 1LBH) and shifted from that found in the coiled-coil modules of other chemotaxis proteins, such as the CheA dimerization domain. The structures of the three known receptors (Tsr_C, $Tm1143_C$, $Tm14_C$) are all very similar in the highly conserved, membrane distal tip that interacts with CheA. However, there is more structural variation among the receptors in the adaptation and flexible bundle region that compose the helical stalks.

Helical bundle parameters, calculated with HELANAL (*39*), reveal substantial distortions and asymmetry in Tm14. HELANAL calculates vectors fit to four successive C-alpha positions and defines a local bending angle between neighboring vectors along the helix. If the local bending angle is more than 20 degrees the helix is classified as kinked. Furthermore, the degree to which the origins of the vectors trace a line or a circle classify the helix as linear or curved (*39*). This analysis showed that both subunits (A and B) of $Tm1143_C$ and Tsr_C have kinks throughout their structure. However in $Tm14_C$, subunit A curves for its entire extent, but subunit B kinks at the bulge and then is mostly linear moving down towards the tip (Figure 3.2). This asymmetry is also reflected in the local helical bending angle of subunit A, which does not change substantially, unlike that of subunit B and both subunits of either Tsr_C or $Tm1143_C$. Pulling the two subunits apart reveals that subunit B must become straight after the kink in order to maintain close contact with the continually curved subunit A (Figure 3.3). Not only is there asymmetry among subunits A and B but also among the N-terminal and C-terminal helices. Taking the pitch between parallel sets of helices as an indicator for supercoiling, the C-terminal helices supercoil to a much greater degree (93 Å pitch) compared to the N-terminal helices and typical coiled-coils (150-200 Å pitch) (*40*). Viewed another way, the C-terminal helices have more

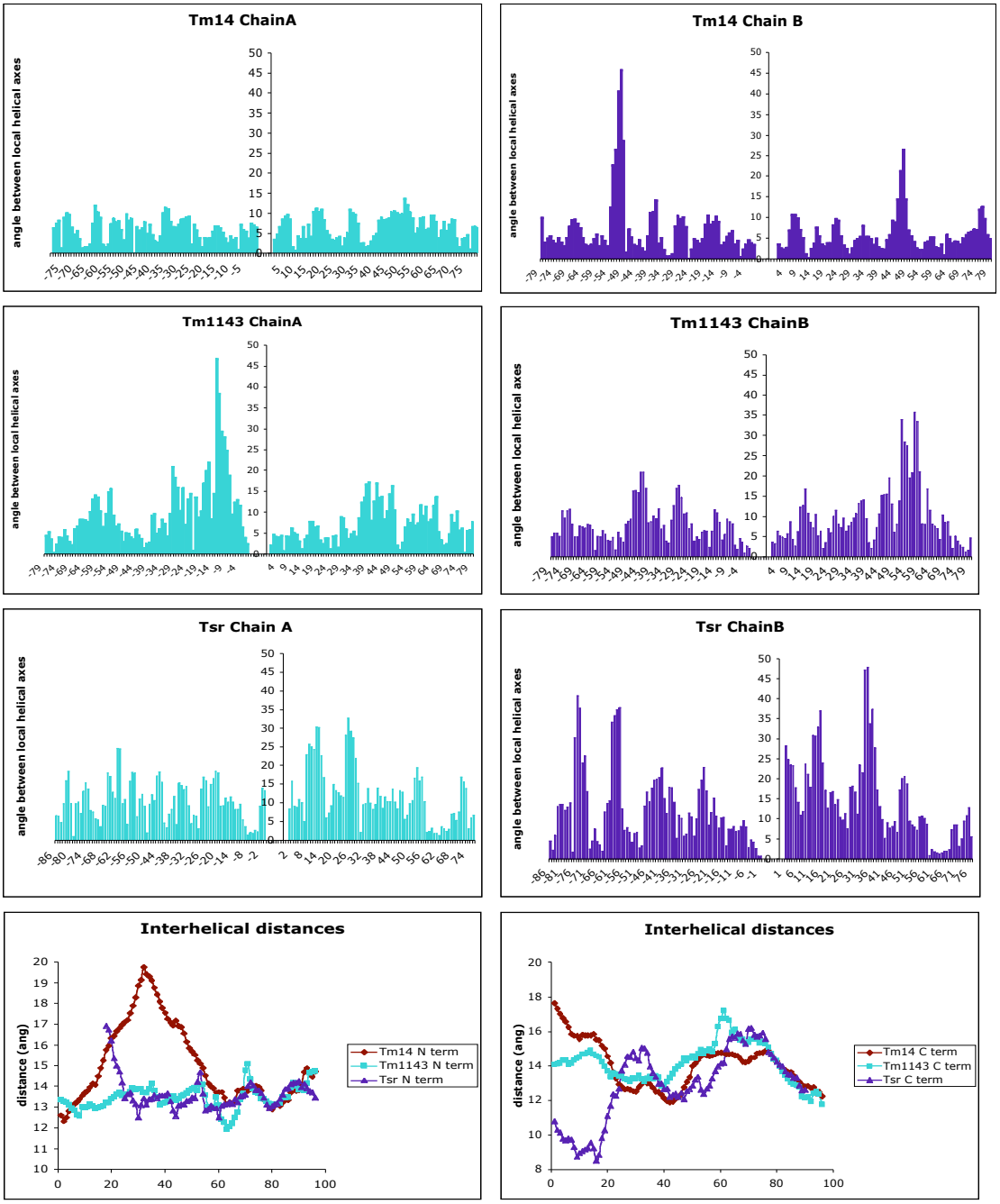

Figure 3.2. Structural parameters of the three receptor structures as analyzed by HELANAL. These parameters further illustrate the asymmetry between the two subunits in Tm14 as compared to Tm1143 and Tsr.

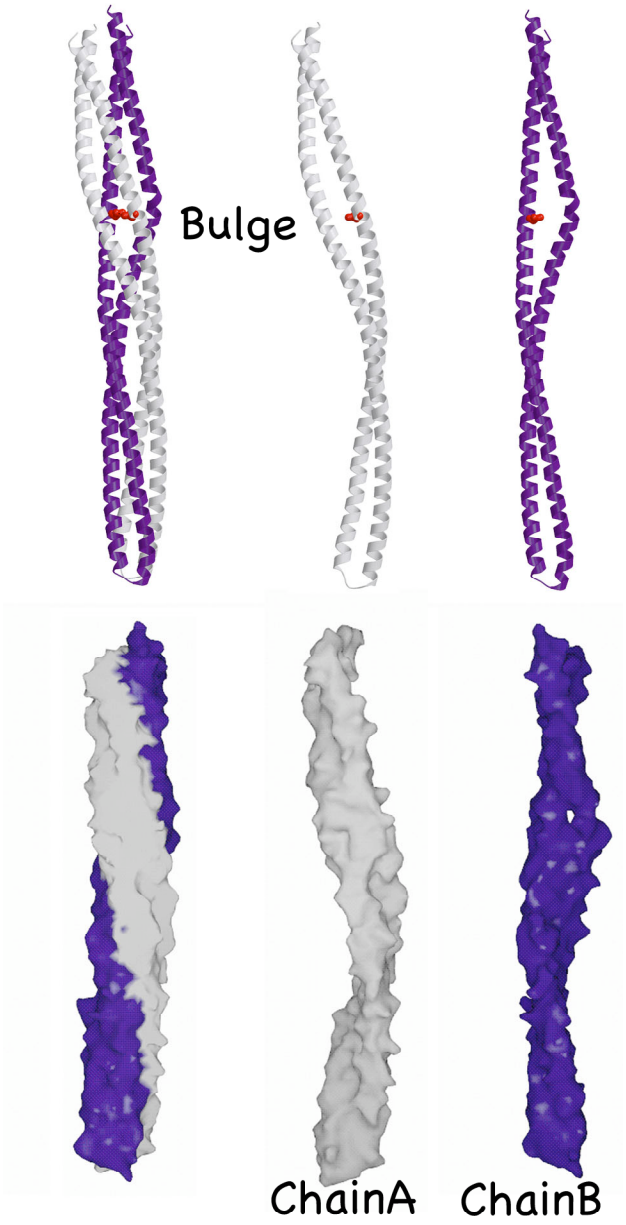

Figure 3.3. Asymmetry between subunits A and B in Tm14. Subunit B is kinked at the bulge, but elsewhere quite linear, whereas subunit A is curved through out its length. The bulge in subunit B makes a solvent accessible gap in the molecular surface.

left-handed twist than the N-terminal helices. To our knowledge, the degree of structural asymmetry in Tm14 is unprecedented for a long 4-helix bundle structure.

The net result of subunit asymmetry resulting from the helical bulge is to shift the conserved signaling tip relative to the flexible bundle region (Figure 3.6). Packing within the conserved region of the tip is regular and very similar to that found in the structures of $Tm1143_C$ and Tsr_C. However, superimposing the helical stalks of Tm14 with either $Tm1143_C$ or Tsr_C reveals that in Tm14 the tip is displaced ~ 25 Å away from its position in the more symmetric receptors. In contrast, if one superimposes the conserved tips, the stalks spread out by about 20 Å. In either case, large motions of the regions known to interact with CheA and CheW, or the modification enzymes may have functional relevance.

The greatest degree of asymmetry between the Tm14 subunits localizes in the aforementioned bulge 108 Å from in the signaling tip. Here, the side chains of Met77A and Met77B in the *d* positions on the N-terminal helices move away from the center of the bundle, whereas the corresponding *d* residues on the C-terminal helix, Asn217A and B, direct their side chains at each other and hydrogen bond across the bundle core. Although, most *d* positions of chemoreceptors hold hydrophobic residues, nearly all MCP sequences contain at least one hydrophilic *d* residue. In Tm14, the Asn217 interaction forms an "x-layer", as defined by (*41*), in which the two Cα-Cα bonds point at each other and are nearly in the same plane (Figure 3.7). The polar Asn side chains also likely facilitate the penetration of ordered solvent into the bundle core.

The pinching together of Asn217 A and B displaces the N-terminal helices outward and forms a prismatic structure in cross-section (Figure 3.7). At the periphery of the bulge, Asp76B breaks from helical geometry to the greatest degree and has larger thermal (B) factors than nearby residues. The Asp76B carbonyl oxygen points out from the helix and is 5.1 Å from what would be its i+4 hydrogen-bonding partner, the amide nitrogen of Ile 80 (Figure 3.4).

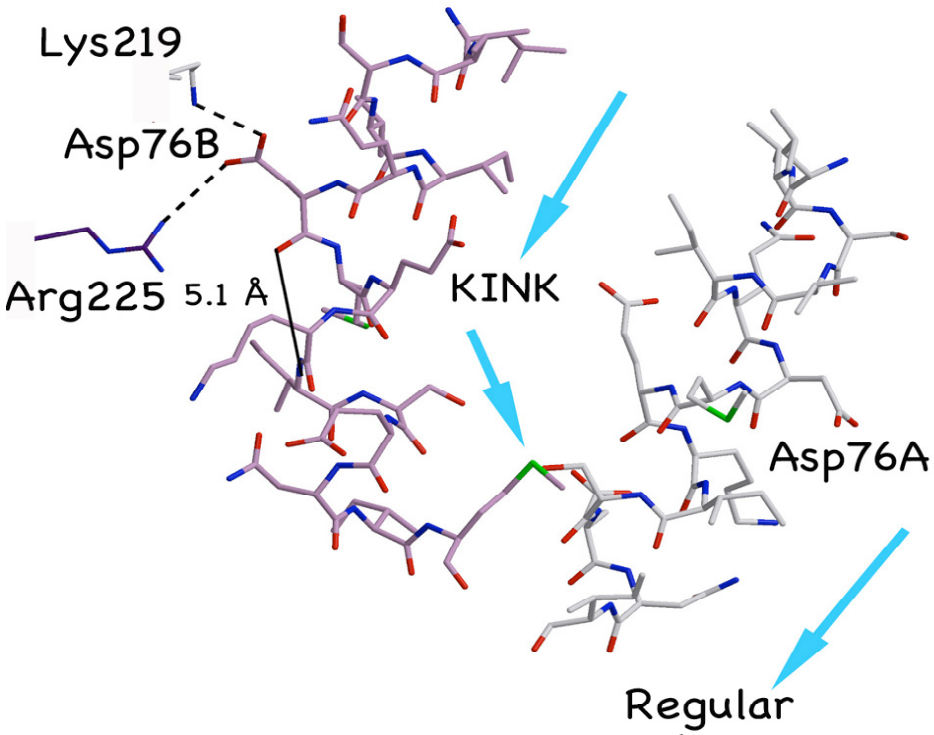

Figure 3.4. Close-up of the bulge distortion. The kink at Asp76B generates a 45 degree change in the direction of the helical axis. Interactions of Asp76 correlate with local helix unwinding in subunit B. Asp76B breaks peptide hydrogen bonding within the helix, but the side chain forms salt bridges with two positively charged residues on different dimers in the crystal lattice. Arrows show directions of the individual helical axes.

Notably, the charge on Asp76B is at least partially neutralized through salt bridges with Lys 219A and Arg 225B on neighboring dimers in the crystal lattice (Figure 3,4). In contrast, Asp 76A does not form a salt bridge with symmetry related dimers, maintains regular helical packing, and unlike Asp76B, has low B factors consistent with the rest of the structure. Charge compensation at an aspartate is interesting because Asp76 is positioned analogously to Glu residues in other MCPs that are known to undergo neutralization by the methylation reactions of the adaptation response. Thus, the crystal contacts provided by Lys219A and Arg225B may be a chemical analogy to methylation and have thereby serendipitously promoted a distortion normally caused by the biologically relevant mechanism of charge neutralization. It is worth noting that because the interactions between molecules in the lattice are extensive (as they also are for the other MCP_C structures), we cannot rule out additional influences of crystal packing on the $Tm14_C$ conformation. Nonetheless, these domains are situated close to each other in the receptor arrays and thus their modes of interaction, as demonstrated in the crystal lattice are of interest.

To test the importance of hydrogen-bonding within the helix core for stabilizing the Tm14 distortion, the Asn217 residues were mutated to Ile, a common *d* position residue. Crystals of the Asn217Ile $Tm14_C$ grew under similar conditions and were isomorphous with those derived from the wild-type (wt) sequence, but diffracted to much lower resolution (3.0 Å, Table 3.1). The structure of the variant is similar to that of the wt in the region of the bulge with the Ile217 residues forming van der Waals contacts across the bundle core (data not shown). However, increased thermal factors and less discernible electron density indicate considerably more disorder in the Ile

variant structure. Thus, under this crystallization condition and in this lattice environment, buried Asn residues are not necessary to form a bulge. Nonetheless, the energetic penalty for not satisfying the Asn hydrogen bonds in the bundle core makes it likely that these residues promote the distorted conformation in the context of the wt sequence.

Crystal packing interactions provide some information for how MCP_Cs will interact with each other when at high concentrations. For one dimension of the crystal lattice, the Tm14 receptors stack in hedgerows, much like those found in the structure of $Tm1143_C$. However, the hedgerow stacking includes the tip distortion, such that all of the aligned receptors bend in the same direction. Neighboring hedgerows associate head-to-tail with interactions between neighboring dimers mediated by salt bridges between highly conserved residues that flank the signaling tip. Arg131A and Arg146B on one dimer interact with Glu149B and Glu160B on another, respectively. Arg146, Glu149, and Glu160 are strictly conserved in chemoreceptors (*8*) and their salt bridges bring two receptor tips into a close-packed interface of 633 $Å^2$ of buried surface area per dimer (Figure 3.5). Arg131 lies at the beginning of the highly conserved region and this residue position mediates receptor-to-receptor contacts in the other two MCP structures. In Tsr_C this residue is a Phe involved in the trimer interface (*21*, *42*) whereas in $Tm1143_C$ this residue is a Glu (presumably protonated) which interacts with its symmetry mate in an aligned neighboring dimer (*23*). All the other *T. maritima* transmembrane receptors including Tm1143 have a Glu in this position, only the soluble Tm14 has an Arg. In the Tm14 structure, the conserved Glu and Arg residues align the respective tips in an anti-parallel configuration, which would be a

permitted association mode for a soluble receptor, and also for a transmembrane receptor in the context of a membrane invagination (*26*).

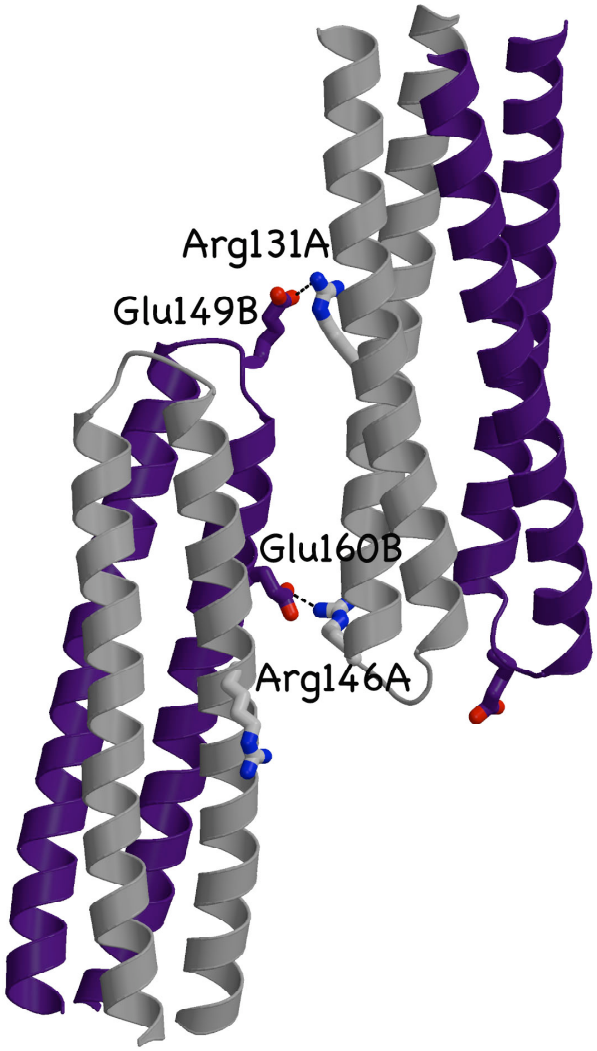

Figure 3.5. Head-to-tail crystal packing interactions of Tm14 within the crystal lattice. Strictly conserved residues Arg146 , Glu149, and Glu160 are involved in salt bridges to an adjacent dimer in the crystal lattice. These salt bridges bring the signaling tips of the receptors close together.

3.4 Discussion

The overall conformation of the receptor dimer is much more distorted in Tm14 than in $Tm1143_C$. These structural differences may derive from the

higher crystallization pH of Tm14 compared to $Tm1143_C$, which produced crystals at low pH where most of the surface acid groups were likely neutralized (*23*). Structures of Tsr_C that had two Glu residues replaced Gln to mimic methylation had lower thermal (B)-factors in the adaptation region (*22*). Furthermore, studies of *E. coli* Tar corroborate that removal of negative charge on the receptor surface by residue substitution reduces flexibility; this in turn enhances CheA activation (*43*). Thus, the greater distortions of Tm14 may reflect its increased dynamics under conditions where more surface anionic groups are ionized. Notably, the largest distortion in the Tm14 bundle occurs at a position where a surface Asp (76) salt-bridges to other positively charged residues in adjacent molecules. Thus, neutralization of surface charge in Tm14 correlates with the local unwinding of a helix and disruption of the bundle packing, thereby imparting flexibility to the entire molecule.

Engineering disulfide bridges into the Tar receptor can dramatically affect its ability to regulate CheA. In particular, cross-links at some *d* positions, lock on CheA activity (*44*). These sites are contained in heptads very similar in sequence and position to the Tm14 heptad that forms the bulge containing Asn217 (Figure 3.6). A disulfide bond at the 217 position would bring *d* residues on adjacent subunits even closer together than is achieved by the hydrogen-bonding Asn residues. For a disulfide to form, the C-terminal helices will have to pinch in, and a bulge of the N-terminal helices, as found in Tm14, will likely result (Figure 3.6). Thus, a distortion, not unlike that observed for Tm14 may contribute to the lock-on phenotype.

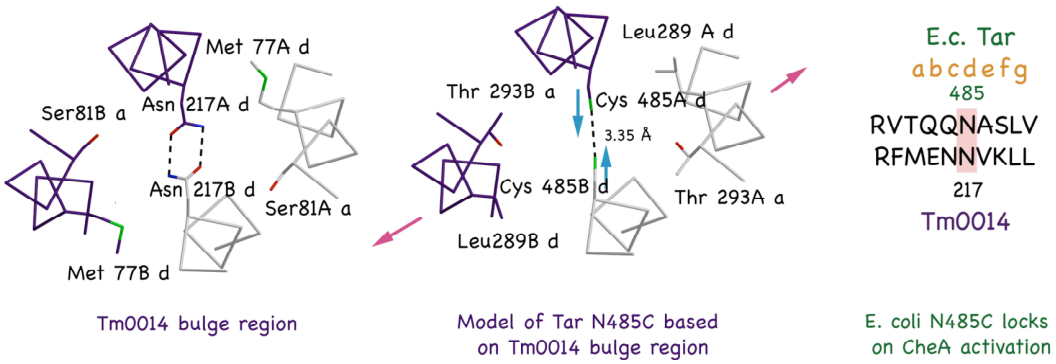

Figure 3.6. Relevance of Tar lock-on disulfide bonds to the bulge distortion of Tm14. Sequence similarity between the heptads in Tar where an engineered Cys cross-link locks on CheA activation and the heptad in Tm14 that forms the bulge (center). Left: Helical packing of Tm14 showing the two internally hydrogen-bonded Asn217 residues. Middle: Model of Tar adaption region where disufide crosslinking locks-on CheA activity. A disulfide bond would generate an even shorter distance between helices and a more prismatic distortion of the bundle core. Right: Sequence alignment of the Tar heptad model with the $Tm14_C$ distortion region.

How then could such local distortions affect the CheA kinase, which binds to the conserved tip over 100 Å away? The kink in Tm14 does not translate to irregular helical packing in the kinase-binding region and the conserved tip is very similar in structure among all of the characterized MCP_Cs. However, what does differ among Tm14, Tsr_C and $Tm1143_C$ is the position of the tip relative to the stalks. The kink in subunit B generates asymmetry between the subunits that manifests over their entire length. As a consequence, the tip swings out, > 25 Å from its comparable position in the

other receptors if the stalks are aligned above the adaptation region (Figure 3.7). Conversely, if the tips are taken as a fixed point and superimposed, the stalks spread ~20 Å. Thus, the $Tm14_C$ structure demonstrates one way a local conformational change in the flexible region high-up in the helical stalks can influence a more static kinase-binding region downstream.

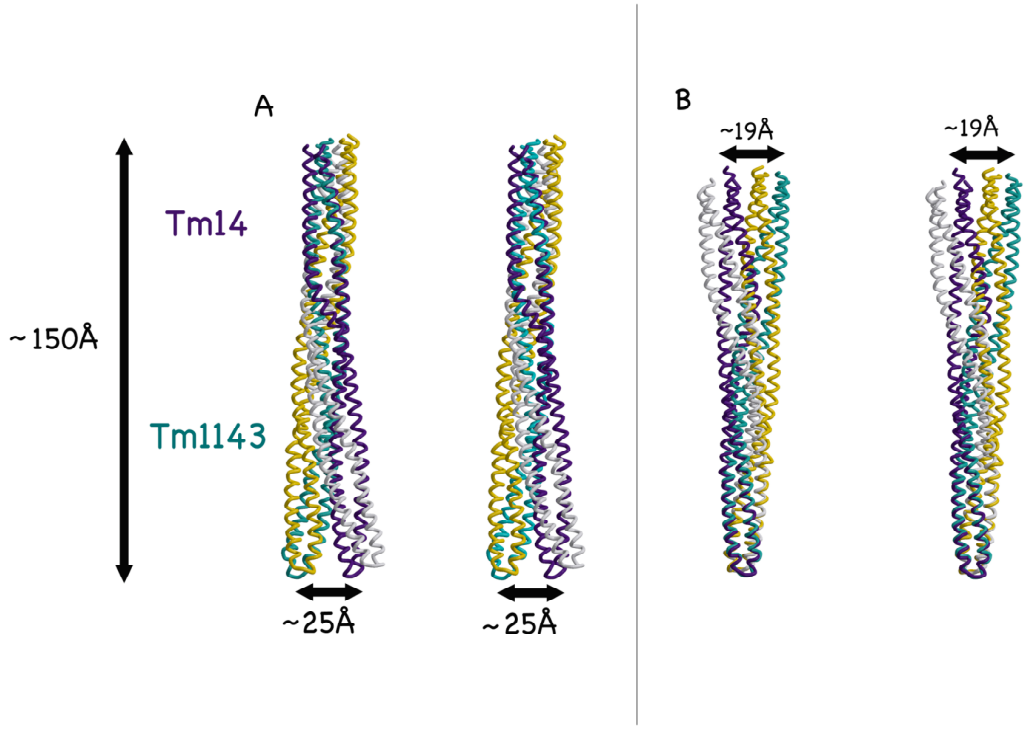

Figure 3.7. The bulge causes displacement of the Tm14 signaling tip relative to the helical stalk. A) Stereoview of the superposition of Tm1143 (light seagreen and gold) and Tm14 (dark purple and light grey) reveal the repositioning of the tip by ~25 Å as a result of a distortion in the helical stalks. Tm1143 represents how Tm14 would appear if both subunits were more symmetric. The C-alpha trace of residues 217-252 of Tm14 superimposed with a RMS of 1.7 Å . B) Stereoview of the 19 Å movement of the stalks if the conserved tips are superimposed (residues 149-164).

Movement of the receptor tip relative to the stalks in $Tm14_C$ derives directly from helical packing irregularities in the bulge. Charge neutralization of Asp76B in the crystal lattice suggests how packing distortions may result from changes in methylation state within the adaptational region, but could such distortions also be propagated from the membrane proximal regions of the receptor in response to ligand binding? It has been proposed that signaling through the HAMP domain involves switching between two nearly isoenergetic helical packing modes related by relative rotations of the helices (*9*). Instead of "knobs-into-holes" packing typical of coiled coils, the HAMP domain structure has "knobs-into-knobs" packing that generates so-called complementary x-da layers (Figure 3.7). In a canonical coiled-coil, the *a* and *d* residues pack into the core symmetrically and equally. Nonetheless, most coiled coils of length greater than a few heptads show some kind of discontinuity, which can be classified as either a stutter (4-residue insertion into the heptad repeat) or a stammer (3-residue insertion) (*41*). In a stutter, *a* residues point into the center of the core and push the *d* and *e* residues out to form a ring around the core. In a stammer, *d* residues point into the center of the core and the *a* and *g* residues form the ring around the core. An "x-layer" is formed from residues that point into the core, whereas a "da-layer" forms from residues in the peripheral ring ((*41*) and Figure 3.7). Such discontinuities can impart flexibility and may generate the structural specificity needed to discriminate subunit interactions among different types of receptors

The HAMP domain is thought to toggle between knob-into-holes packing and complementary x-da packing through a rotation induced from signals sent through the membrane (*9*). Surprisingly the structure of Tm14 assumes a variety of packing modes at different positions along its length,

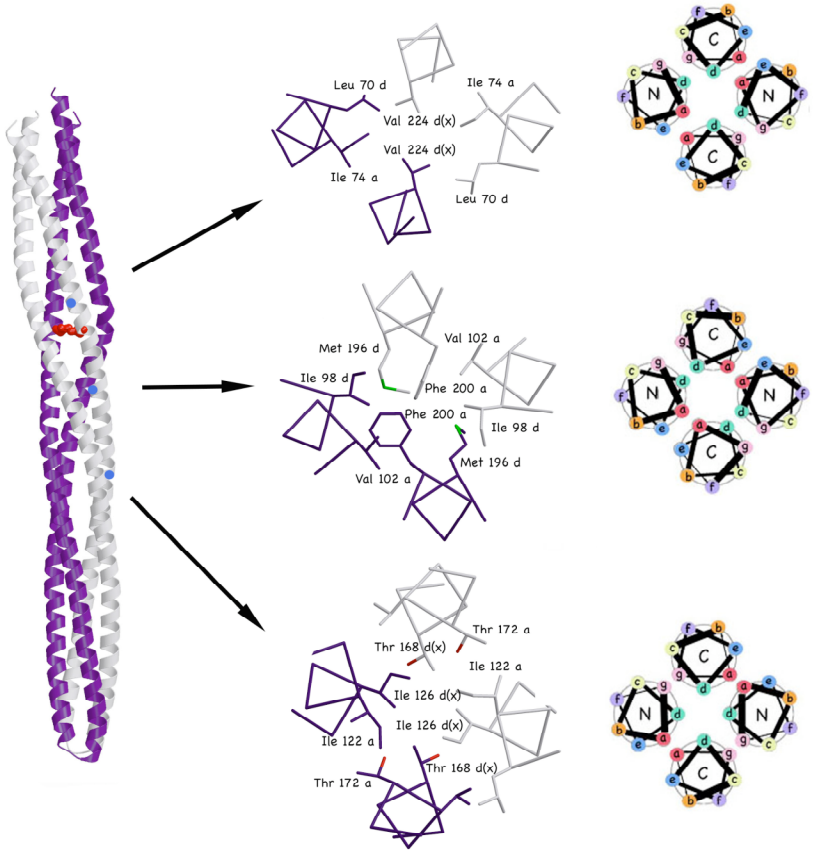

Figure 3.8. Variations in helical packing in different positions throughout the Tm14 structure. Subunits A and B shown in gray and purple, respectively. The heptad is represented by sites *a-f* in the helical wheel formation. The helical packing in the Tm14 structure is not regular but varies significantly across the length of the receptor. Top: mixed x-da layers packing; Center: da-layer packing; Bottom: x-layer packing.

including the two proposed for the signaling states of the HAMP (Figure 3.8). In general most of the C-terminal helices are in the x position where in the N-terminal helices the da position dominates. However, the C-terminal helices become more x-like moving away from the tip, whereas the N-terminal helices become more x-like down toward the tip. In the bulge, a da configuration of

the N-terminal helices allows the C-terminal helices to form a highly prismatic x-layer in which the Asn217 residues make close contact. Outside the flexible bundle region of Tm14 and in all of $Tm1143_C$ the packing is mostly symmetric x-layers, staggered by 0.25 of a heptad. Such pure x-layer packing is incompatible with the bulge distortion of Tm14 because of steric hindrance from the core residues in the layers above and below. However, it seems likely that in solution the helical packing in Tm14 may fluctuate to a more symmetric x configuration. The different packing arrangements observed in the MCP_C structures over their length, despite very similar sequence contexts suggests that their structures can readily change. Thus, forces that influence local helix interactions within the coiled-coil, perhaps exerted by conformational change within the HAMP domain or transmembrane region could have a substantial impact on the overall receptor conformation.

The Tm14 structure indicates that changes in local helical packing, mediated by x-da layers, can be readily translated into bending of the stalks and translation of the conserved tip. This amplification of spatial displacement at the tip derives directly from the length of the receptor, the position of the distortion and coupling among the main structural parameters that ultimately determine coiled-coil conformation. FRET studies of Tsr-YFP fusions suggest that activating ligands induce substantial bending motions in the receptor stalks (*45*). Furthermore, genetic studies of Tsr that introduced mutations into the signaling region showed that prolines (as opposed to Trp or Ala residues) were the most devastating for clustering, kinase activation and ternary complex assembly (*42*). Proline residues generate kinks in helices and may thereby distort the position and/or conformation of the tip. Similarly, replacements at conserved Gly residues in the helical stalks of the *E.*

coli receptors has dramatic effects on CheA activation (*46*). The inherent flexibility of Gly residues may facilitate tip-bending distortions. Indeed, distortions in $Tm1143_C$ from regular helical packing often localize at Gly residues.

Overall, the structure of Tm14 reveals a new MCP_C structural state that provides possible explanations for how changes in packing and surface properties within the receptor stalk can reposition the kinase-activating tip (Figure 3.7A). Such local distortions could arise from modification in the adaptation region and/or packing rearrangments induced by the HAMP domain. If the distortions observed in $Tm14_C$ are important for receptor function we are left with the possibilities of either the stalks remaining fixed and the tip moving, visa versa, or some combination of both. Because CheA and CheW bind the tip, it seems likely that this interaction region must in some way change structure or position to relay signals to the kinase. If the tips were to remain fixed in all signaling states of the receptor and the major conformational changes were in the stalk region, it is not evident how the kinase would be impacted. However, a recent study of cryo-electron tomograms of overexpressed Tsr chemoreceptors finds two primary structural states: 1) an expanded trimer of dimers (CheA inhibiting) and 2) a compact trimer-of-dimers (CheA activating). These states differ mainly by movement of the HAMP domains by 25 Å in a plane roughly perpendicular to the trimer axis. If we superimpose the distortion in Tm14 onto Tm1143 this time with the assumption that the tips always remain associated by the trimer contact then the difference in distance between the start of the adaptation region is about 11 Å (Figure 3.7B), which on extrapolation up toward the membrane would be consistent with a 25 Å difference at the HAMP domains (*47*). This

study also observed that the expanded form results in an 8% reduction in the height of the trimers (*47*). It seems plausible that this height reduction might result from a bending or tilting of the individual dimers in the trimer formation. Thus although the precise mechanism by which conformational changes in the receptor trimers affect CheA remain unresolved, flexing of the helical stalks and repositioning of the receptor tips are likely to play an important role.

Finally we note that the $Tm14_C$ structure is highly asymmetric. If the receptors contained within the signaling arrays are in contact with each other, there may be a strong tendency for them to distort together in one direction. Thus, the swinging motion of the tip could reorganize interactions among receptors, CheA, and CheW in a highly cooperative manner.

Why would the chemoreceptors contain discontinuities given the stability of the knobs-into-hole packing? Deviations from the heptad repeat might exist simply because it does not interfere with the function of the four-helix bundle. Because perfect knobs-into-hole packing was not essential to function it was not conversed in the receptor. However, it is possible that discontinuities found in the receptor structures are not a fluke but critical to function. From the HAMP domain NMR structure the ability to switch from canonical to noncanonical is proposed to be the mechanism by which the HAMP domain transmits a signal (*9*). If structural variations are important for signaling what sort of advantages are conferred by the receptor containing discontinuities.

One advantage of having noncanonical coiled coils is that the helical register is maintained. With only heptads two core positions would be exposed to solvent with the helices off register (*48*) (Figure 3.9). In the case of

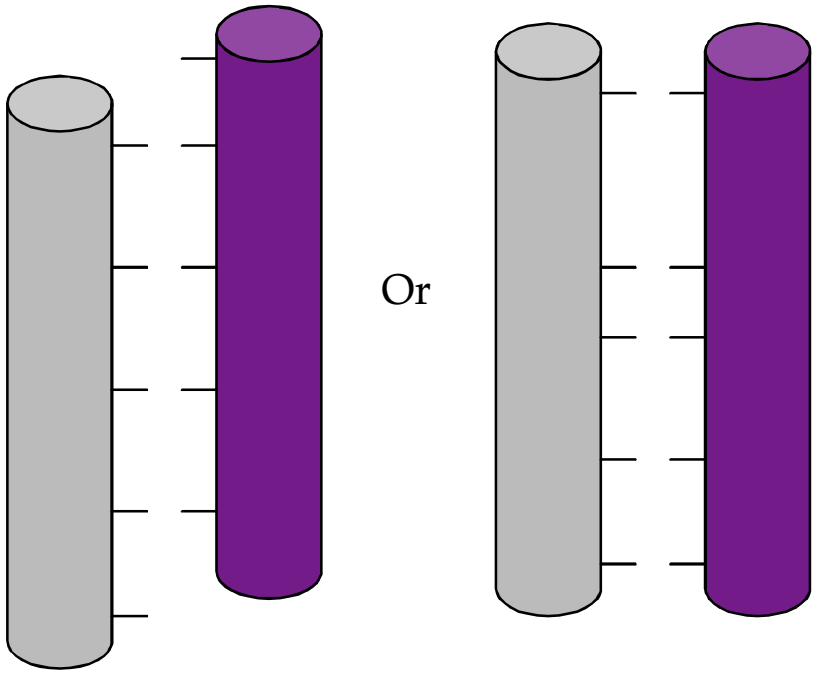

Figure 3.9. Illustration of how discontinuities maintain helical register. On the left is a dimer composed of only heptad repeats. In this dimer the helices slip relative to each other but a still able to maintain most of the hydrophobic contacts. The dimer on the right has discontinuities if the helices slip relative to each other the majority of favorable contacts would be lost. Thus discontinuities are better able to maintain the precise register of the helices.

discontinuities it is less likely that the helices would become out of register because more than two positions would be lost in terms of favorable hydrophobic contact. If the mechanism of signaling involves a slight piston motion with a low energy barrier discontinuities could ensure that the helices return to the correct register once the signal is gone. This could be particularly

important with the abundance of hydrophobic residues in the receptor often times there are hydrophobic residues in the "g" and "e" positions as well.

Another advantage of the chemoreceptor containing discontinuities is it allows for a change in stability without changing the oligomeric state (*48*). Chemotaxis requires a fast transmission of information for a quick response time it seems that this would be harder to deliver if the entire dimer over 300 Å long had to break in order to transmit a signal. Having the receptor as a highly stable coiled coil might also make it difficult to transmit a signal in that it might set the energy barrier too high for a change in structure to be propagated down the receptor. Discontinuities give the receptor a bit of instability in that the interactions are not as stable as knobs-into-holes, which could be important for signal transmission (Figure 3.10). Alteration of the knobs-into-holes packing that generates various discontinuities is a way of imparting controlled flexibility to certain regions of the receptor.

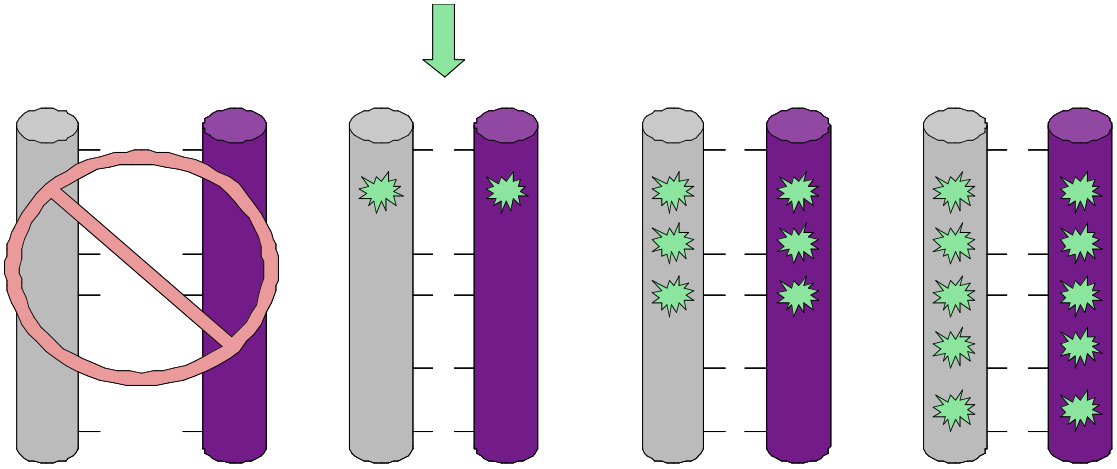

Figure 3.10. Illustration of how discontuities aid signaling. Changes in oligomeric state on the left would have a high energy barrier. If the signal is transmitted down the dimer and the heptad is very stable it would be unfavorable to have a signal that required a disruption of the heptad interactions to be propagated. However if the dimer contained less stable discontinuities the impart flexibility it might make changes in helical packing to propagate the signal more favorable.

From the three crystal structures it would seem that the packing of the tip is rather stable and rigid given that all three crystal structures have identical interhelical distances in the signaling tip (Figure 3.2). In the signaling region the internal residues as well as the external residues are strictly conserved. Presumably the internal residues that are strictly conserved and do not interact directly with CheA and CheW but are conserved to maintain the internal packing of the receptor. Perhaps internal packing must be maintained in the signaling region for a reason. Mutations of the internal residues also affect signaling therefore coiling of helices (internal residues contacts) should be important in signaling. Furthermore, cross-linking studies have shown that not all internal residues affect signaling when mutated to a cysteine and cross-linked (*44*) indicating that in specific parts of the receptor certain helical packing is more important than other parts. The specificity of internal mutations affecting signaling supports the idea that discontinuities are important for function. With only heptad positions influencing the structure, one would expect the effect of mutations to be more uniform along the length of the receptor. The sequence among chemoreceptors in the same organism can be quite different even in the cytoplasmic region. Probably only the ligand-binding domain would have to be very different, but the cytoplasmic part could be almost identical. In the *T. maritima* genome there are three transmembrane receptors that are nearly identical in their cytoplasmic sequence and three that are unlike any others in the cytoplasmic sequence. It is possible that the reason the sequences might vary is because of carefully imparted discontinuities. The difference in

sequence could influence the sensitivity of the cell to certain extracellular ligands. Sequence variation away from the tip might be a strategy rather than an accident.

3.5 Conclusions

In this work we have measured the stoichiometry of the ternary signaling complex from *T. maritima*, tested its activity and solved the structure of one of its main components the soluble receptor, Tm14. In our experiments there was no evidence of the higher order trimer of dimers structure as seen in the well-characterized *E. coli* system. These results seem to indicate that perhaps the signaling unit in *T. maritima* is different than E. coli. However recent cryo-EM images, (communication with Adriane Briegel) that are soon to be published, reveal that *T. maritima* along with several other species of bacteria contain the hexagonal pattern that is present in E. coli (Figure 3.11). These images present a strong argument for a trimer of dimers *in vivo*, even in the *T. maritima* organism whose signaling unit we set out to characterize with our soluble *in vitro* system.

Given the current strong evidence for an *in vivo* trimer of dimers is there anyway to rationalize our *in vitro* findings with the *T. maritima* proteins. One possible rationalization might be found in the function of the soluble chemoreceptor, Tm14. In the absence of *in vivo* experiments most of what we can say about the function of the Tm14 is speculative. It has no obvious sensing domain so it is unlikely that is sensing something internal inside the cell as has been proposed for other soluble receptors with PAS domains. Perhaps the function of Tm14 might be to organize the receptors of T. maritima into trimers. This idea is supported by the fact that a small soluble

receptor, which also appears to lack a sensing domain, when removed from *Borrelia Burgdorferi* renders the organism completely non-chemotactic.

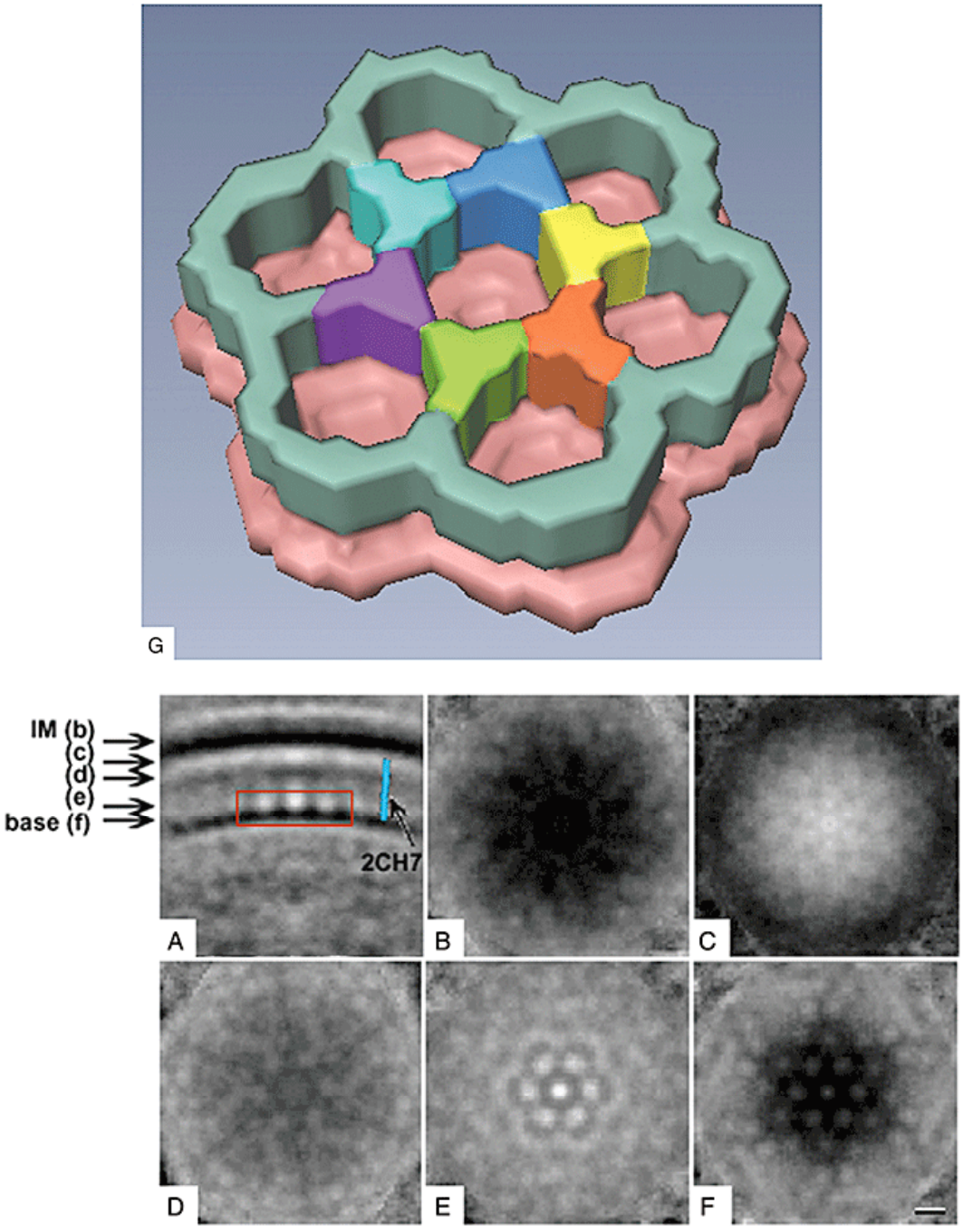

Figure 3.11 Hexagonal arrangement of chemoreceptors in the membrane imaged by cryo-EM. Model of hexagonal arrangment (top). Actual cryo-EM of bacterial chemoreceptors (bottom). These figures are borrowed from Briegel et al. Mol. Microbiol. 2008, **69**:30-41

Tm14 has many more exposed positively charged residues residues than the transmembrane receptors. The N-terminal overhang of Tm14 has a high density of lysines and arginines. This overhang is in the same area as the negatively charged glutamates in the adaptation region making it favorable to pack against the transmembrane receptors. Another way to explain the discrepancy between the in vivo hexagonal arrangements and the vitro work presented here is that perhaps we have characterized only the inhibitory state of the receptor. In the EM images there are also receptor patches that are arranged in hexagons but with more disordered arrays. Perhaps our in vitro system is consistent with the disordered arrays. Maybe the in vitro stoichiometry of one CheA dimer: one receptor dimer: two monomers of CheW is simply the inhibitory state of the signaling unit and the activated state is found in the ordered hexagonal arrangement. However, it would seem that in this case the amount of hexagonal arrays versus disordered arrays should vary quite a bit from organism to organism given that in one organism the hexagonal arrays would lead to tumbling (*E. coli*) where as in another organism (*B. subtilis*) it would cause smooth swimming. Even if the *in vivo* arrangement of the chemoreceptor is a trimer of dimers, creating such system *in vitro* has been changing, even with E. coli proteins. Currently we are exploring artificial means to try to generate a soluble trimer of dimers. Hopefully by creating a trimer of dimers with the cytoplasmic fragments of *T. maritima* receptors we will then generate an *in vitro* system to investigate the signaling unit contained within the *in vivo* hexagonal arrays.

REFERENCES

(1) Szurmant, H., and Ordal, G. W. (2004) Diversity in chemotaxis mechanisms among the bacteria and archaea. *Microbiol Mol Biol Rev 68*, 301-19.

(2) Sourjik, V. (2004) Receptor clustering and signal processing in E. coli chemotaxis. *Trends Microbiol 12*, 569-76.

(3) Wadhams, G. H., and Armitage, J. P. (2004) Making sense of it all: bacterial chemotaxis. *Nat Rev Mol Cell Biol 5*, 1024-37.

(4) Parkinson, J. S., Ames, P., and Studdert, C. A. (2005) Collaborative signaling by bacterial chemoreceptors. *Curr Opin Microbiol 8*, 116-21.

(5) Falke, J. J., and Hazelbauer, G. L. (2001) Transmembrane signaling in bacterial chemoreceptors. *Trends Biochem. Sci. 26*, 257-265.

(6) Hazelbauer, G. L., Falke, J. J., and Parkinson, J. S. (2008) Bacterial chemoreceptors: high-performance signaling in networked arrays. *Trends In Biochemical Sciences 33*, 9-19.

(7) Yeh, J. I., Biemann, H. P., Prive, G. G., Pandit, J., Koshland, D. E., and Kim, S. H. (1996) High-resolution structures of the ligand binding domain of the wild-type bacterial aspartate receptor. *Journal Of Molecular Biology 262*, 186-201.

(8) Alexander, R. P., and Zhulin, I. B. (2007) Evolutionary genomics reveals conserved structural determinants of signaling and adaptation in microbial chemoreceptors. *Proceedings Of The National Academy Of Sciences Of The United States Of America 104*, 2885-2890.

(9) Hulko, M., Berndt, F., Gruber, M., Linder, J. U., Truffault, V., Schultz, A., Martin, J., Schultz, J. E., Lupas, A. N., and Coles, M. (2006) The

HAMP domain structure implies helix rotation in transmembrane signaling. *Cell 126*, 929-940.

(10) Swain, K. E., and Falke, J. J. (2007) Structure of the conserved HAMP domain in an intact, membrane-bound chemoreceptor: A disulfide mapping study. *Biochemistry 46*, 13684-13695.

(11) Ames, P., Zhou, Q., and Parkinson, J. S. (2008) Mutational analysis of the connector segment in the HAMP domain of Tsr, the Escherichia coli serine chemoreceptor. *Journal Of Bacteriology 190*, 6676-6685.

(12) Bornhorst, J. A., and Falke, J. J. (2003) Quantitative analysis of aspartate receptor signaling complex reveals that the homogeneous two-state model is inadequate: Development of a heterogeneous two-state model. *Journal Of Molecular Biology 326*, 1597-1614.

(13) Lai, W. C., Beel, B. D., and Hazelbauer, G. L. (2006) Adaptational modification and ligand occupancy have opposite effects on positioning of the transmembrane signalling helix of a chemoreceptor. *Molecular Microbiology 61*, 1081-1090.

(14) Li, G., and Weis, R. M. (2000) Covalent modification regulates ligand binding to receptor complexes in the chemosensory system of *Escherichia coli. Cell 100*, 357-365.

(15) Park, C. Y., Dutton, D. P., and Hazelbauer, G. L. (1990) Effects Of Glutamines And Glutamates At Sites Of Covalent Modification Of A Methyl-Accepting Transducer. *Journal Of Bacteriology 172*, 7179-7187.

(16) Miller, A. S. a. F., J.J. (2004) Side chains at the membrane-water interface modulate the signaling state of a transmembrane receptor. *Biochemistry 43*, 1763-1770.

(17) Draheim, R. R., Bormans, A. F., Lai, R. Z., and Manson, M. D. (2006) Tuning a bacterial chemoreceptor with protein-membrane interactions. *Biochemistry 45*, 14655-14664.

(18) Danielson, M. A., Biemann, H. P., Koshland, D. E., and Falke, J. J. (1994) Attractant-Induced And Disulfide-Induced Conformational-Changes In The Ligand-Binding Domain Of The Chemotaxis Aspartate Receptor - A F-19 Nmr-Study. *Biochemistry 33*, 6100-6109.

(19) Ottemann, K. M., Thorgeirsson, T. E., Kolodziej, A. F., Shin, Y. K., and Koshland, D. E. (1998) Direct measurement of small ligand-induced conformational changes in the aspartate chemoreceptor using EPR. *Biochemistry 37*, 7062-7069.

(20) Ottemann, K. M., Xiao, W., Shin, Y.-K., and Koshland, D. E., Jr. (1999) A piston model for transmembrane signaling of the aspartate receptor. *Science 285*, 1751-1754.

(21) Kim, K. K., Yokota, H., and Kim, S.H. (1999) Four-helical-bundle structure of the cytoplasmic domain of a serine chemotaxis receptor. *Nature 400*, 787-792.

(22) Kim, S. H., Wang, W. R., and Kim, K. K. (2002) Dynamic and clustering model of bacterial chemotaxis receptors: Structural basis for signaling and high sensitivity. *Proceedings Of The National Academy Of Sciences Of The United States Of America 99*, 11611-11615.

(23) Park, S. Y., Borbat, P.P., Gonzalez-Bonet, G., Bhatnagar, J., Freed, J.H., Bilwes, A.M., Crane, B.R. (2006) Reconstruction of the chemotaxis receptor:kinase assembly. *Nat. Struct. Mol. Biol. 13*, 400-407.

(24) Briegel, A., Ding, H. J., Li, Z., Werner, J., Gitai, Z., Dias, D. P., Jensen, R. B., and Jensen, G. J. (2008) Location and architecture of the Caulobacter crescentus chemoreceptor array. *Molecular Microbiology 69*, 30-41.

(25) Zhang, P. J., Khursigara, C. M., Hartnell, L. M., and Subramaniam, S. (2007) Direct visualization of Escherichia coli chemotaxis receptor arrays using cryo-electron microscopy. *Proceedings Of The National Academy Of Sciences Of The United States Of America 104*, 3777-3781.

(26) Khursigara, C. M., Wu, X. W., and Subramaniam, S. (2008) Chemoreceptors in Caulobacter crescentus: Trimers of receptor dimers in a partially ordered hexagonally packed array. *Journal Of Bacteriology 190*, 6805-6810.

(27) Bardy, S. L., and Maddock, J. R. (2005) Polar localization of a soluble methyl-accepting protein of Pseudomonas aeruginosa. *J Bacteriol 187*, 7840-4.

(28) Wadhams, G. H., Martin, A. C., Porter, S. L., Maddock, J. R., Mantotta, J. C., King, H. M., and Armitage, J. P. (2002) TlpC, a novel chemotaxis protein in Rhodobacter sphaeroides, localizes to a discrete region in the cytoplasm. *Molecular Microbiology 46*, 1211-1221.

(29) Bilwes, A. M., Alex, L. A., Crane, B. R., and Simon, M. I. (1999) Structure of CheA, a signal-transducing histidine kinase. *Cell 96*, 131-141.

(30) Otwinowski, Z., and Minor, W. (1997) Processing of X-ray diffraction data collected in oscillation mode. *Macromolecular Crystallography, Pt A 276*, 307-326.

(31) Kabsch, W. (1993) Automatic Processing Of Rotation Diffraction Data From Crystals Of Initially Unknown Symmetry And Cell Constants. *Journal Of Applied Crystallography 26*, 795-800.

(32) Terwilliger, T. C., and Berendzen, J. (1999) Automated MAD and MIR structure solution. *Acta Crystallographica Section D-Biological Crystallography 55*, 849-861.

(33) Terwilliger, T. C. (2000) Maximum-likelihood density modification. *Acta Crystallographica Section D-Biological Crystallography 56*, 965-972.

(34) Terwilliger, T. C. (2003) Automated main-chain model building by template matching and iterative fragment extension. *Acta Crystallographica Section D-Biological Crystallography 59*, 38-44.

(35) McCoy, A. J., Grosse-Kunstleve, R. W., Adams, P. D., Winn, M. D., Storoni, L. C., and Read, R. J. (2007) Phaser crystallographic software. *Journal Of Applied Crystallography 40*, 658-674.

(36) Brunger, A. T., Adams, P. D., Clore, G. M., DeLano, W. L., Gros, P., Grosse-Kunstleve, R. W., Jiang, J. S., Kuszewski, J., Nilges, M., Pannu, N. S., Read, R. J., Rice, L. M., Simonson, T., and Warren, G. L. (1998) Crystallography & NMR system: A new software suite for macromolecular structure determination. *Acta Crystallographica Section D-Biological Crystallography 54*, 905-921.

(37) Christopher, J. A., and Baldwin, T. O. (1998) SPOCK: Real-time collaborative molecular modelling. *Journal Of Molecular Graphics & Modelling 16*, 285-285.

(38) Gernert, K. M., Surles, M. C., Labean, T. H., Richardson, J. S., and Richardson, D. C. (1995) The Alacoil - A Very Tight, Antiparallel Coiled-Coil Of Helices. *Protein Science 4*, 2252-2260.

(39) Bansal, M., Kumar, S., and Velavan, R. (2000) HELANAL: A program to characterize helix geometry in proteins. *Journal Of Biomolecular Structure & Dynamics 17*, 811-819.

(40) Strelkov, S. V., and Burkhard, P. (2002) Analysis of alpha-helical coiled coils with the program TWISTER reveals a structural mechanism for stutter compensation. *Journal Of Structural Biology 137*, 54-64.

(41) Lupas, A. N., and Gruber, M. (2005) The structure of alpha-helical coiled coils. *Fibrous Proteins: Coiled-Coils, Collagen And Elastomers 70*, 37-+.

(42) Ames, P., Studdert, C. A., Reiser, R. H., and Parkinson, J. S. (2002) Collaborative signaling by mixed chemoreceptor teams in Escherichia coli. *Proc Natl Acad Sci U S A 99*, 7060-5.

(43) Starrett, D. J., and Falke, J. J. (2005) Adaptation mechanism of the aspartate receptor: Electrostatics of the adaptation subdomain play a key role in modulating kinase activity. *Biochemistry 44*, 1550-1560.

(44) Winston, S. E., Mehan, R., and Falke, J. J. (2005) Evidence that the adaptation region of the aspartate receptor is a dynamic four-helix bundle: Cysteine and disulfide scanning studies. *Biochemistry 44*, 12655-12666.

(45) Vaknin, A., and Berg, H. C. (2007) Physical responses of bacterial chemoreceptors. *Journal Of Molecular Biology 366*, 1416-1423.

(46) Coleman, M. D., Bass, R. B., Mehan, R. S., and Falke, J. J. (2005) Conserved glycine residues in the cytoplasmic domain of the aspartate receptor play essential roles in kinase coupling and on-off switching. *Biochemistry 44*, 7687-7695.

(47) Khursigara, C. M., Wu, X. W., Zhang, P. J., Lefman, J., and Subramaniam, S. (2008) Role of HAMP domains in chemotaxis signaling by bacterial chemoreceptors. *Proceedings Of The National Academy Of Sciences Of The United States Of America 105*, 16555-16560.

(48) Hicks, M. R., Holberton, D. V., Kowalczyk, C., and Woolfson, D. N. (1997) Coiled-coil assembly by peptides with non-heptad sequence motifs. *Folding & Design 2*, 149-158.

APPENDIX

A.1 Introduction

The signal in chemotaxis begins with the ligand binding the extracellular domain of the chemoreceptor. It is clear that the binding of the ligand must result in a conformational change in the ligand-binding domain that is propagated down the length of the receptor. Much work as been done to investigate the ligand-binding domain of *E.coli*. The atomic structure of the extracellular domain in E. coli revealed a four helix-bundle subunit (*2*) that form a dimer of eight helices (Figure A1.). Although the receptor is a dimer it is thought that only one subunit is occupied by ligand at a time (*1*). Of the four helices only one extends the entire length of the receptor, α4, it leads into transmembrane helix 2 (TM2) then a linker then the cytoplasmic domain (Figure A2.). Cross-linking and NMR studies have indicated that ligand binding changes the α1/TM1-α4/TM2 interface, but not the dimer interface (α1/TM1-α1′/TM1′) (*3-5*). In the X-ray crystal structure of the extracellular domain of Tar from *E. coli* with its ligand (aspartate) bound, the ligand interacts with residues on the α4 helix (*6*). These combined data have led to the model that ligand binding induces a piston like displacement of the α4 helix to transmit the signal through the receptor. As with other aspects of chemotaxis there are data to suggest that this *E. coli* model may not apply to other bacteria species with different chemotaxis systems.

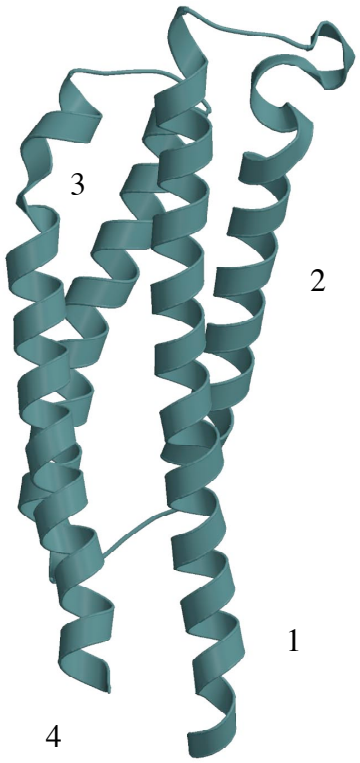

Figure A1. Four helix bundle structure of extracellular domain of the aspartate receptor. Helices labeled 1-4.

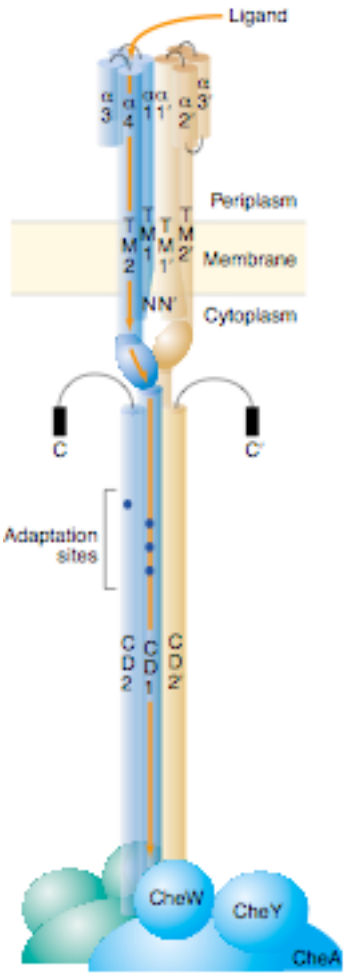

Figure A2. Full length schematic of chemoreceptor. Piston motion model of helix α4 illustrated by orange arrow goes down the length of the receptor (*1*). This figure is borrowed from a review by Falke and Hazelbauer, TiBS, 26, 257-265.

First, the structure of the extracellular domain for many other bacteria, including *T. maritima* and *B. subtilis*, is not predicted to be a four-helix bundle. In fact the extracellular ligand-binding domain of many species is a PAS-like fold recently classified as a CACHE domain (Figure A3.)(*7*). Furthermore, crosslinking studies of the McpB receptor, a *B. subtilis* receptor that binds asparagines, reveals that residues along the TM1-TM1' interface change relative to each other (*8*). The mechanism of ligand binding for the *B. subtilis* receptor extracellular domain is unknown. I set out to obtain a crystal structure of the extracellular ligand-binding domain of *B. subtilis* with ligand bound and ligand unbound. This task was more challenging than anticipated and the structure remains undetermined the following provides the data collected and why structural determination is challenging with the current data.

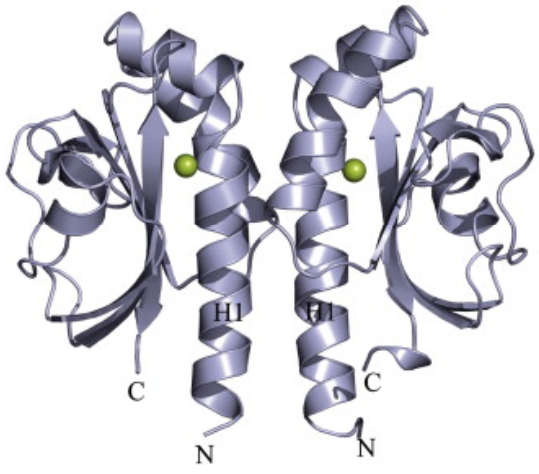

Figure A3. Structure of part of the CACHE domain from CitA (*9*). It is thought that this structure will be very similar to part of the CACHE domain of McpB and C of *B. subtilis*. The other part of the domain should be composed of another β-sheet that makes a strand dyad (*7*).

A2. Methods

Constructs of the McpB N-terminus and one construct of McpC were cloned into pGEX2T by George Glekas of the Ordal lab. Three different constructs of McpB N-term (Ser35 to Ser279), McpB 227 (Gly42 to Ser279) and McpB 229 (Gly42 to Lys274). All three constructs were set up for crystallization but there was no difference observed in terms of crystallization conditions or the type of crystals formed. There were 3 hits out of the Hampton screen all three were screened around to improve the quality of the crystals. Only one condition eventually yielded diffraction quality crystals, 35% PEG 400 - pH 5.4 - 0.1 M $CdCl_2$. These crystals were small (100 microns) and diffracted to 3.5 Å using the additive sodium malonate improved the diffraction as well as the size of the crystals (400 microns). The McpC N-terminal construct crystallized under different conditions 25% PEG 4000 – pH 5.6. The crystals of McpC looked good, but were fragile and too thin (10-20 microns). Seeding into 17% PEG 4000 improved the appearance of the crystals but the diffraction was never better than 4.0 Å. Three data sets were collected of the McpC N-terminus crystals and over 20 data sets were collected of Mcp B N-terminus. Both the crystals of McpB and crystals of McpC were twinned and exhibit pseudo-symmetry but in different ways. A molecular replacement solution was attempted using the *Vibrio cholerae* cache domain structure and a model structure of McpB based on secondary structure predictions. Because molecular replacement did not generate a solution selenomethionine protein was prepared with the intention of using the anomalous scattering signal to determine the phase. However the twinning has potential to corrupt the anomalous signal and then phase could not be determined from selenomethionine data.

The next step was to try to use heavy metals to solve the structure. Heavy metal co-crystallization had the potential to eliminate the twinning by perhaps favoring one conformation of the molecule over another. The original constructs lacked cysteines, which are favorable for binding certain metals, therefore mutants with a cysteine on the predicted -sheet were created. One of the cysteine mutants produced crystals in the presence of Hg compounds. Examination of the Friedel pairs revealed that a difference that might indicate an anomalous signal however the Patterson map did not contain a strong peak to confirm the presence of Hg. Unfortunately the data set collected on crystals grown in the presence of Hg compounds were also twinned this could be due to weak incorporation of the Hg or maybe Hg does not have much a affect on the conformation. The follow is a summary of the some of the data collected on the McpB N-terminus in pursuit of an atomic resolution structure for this interesting domain.

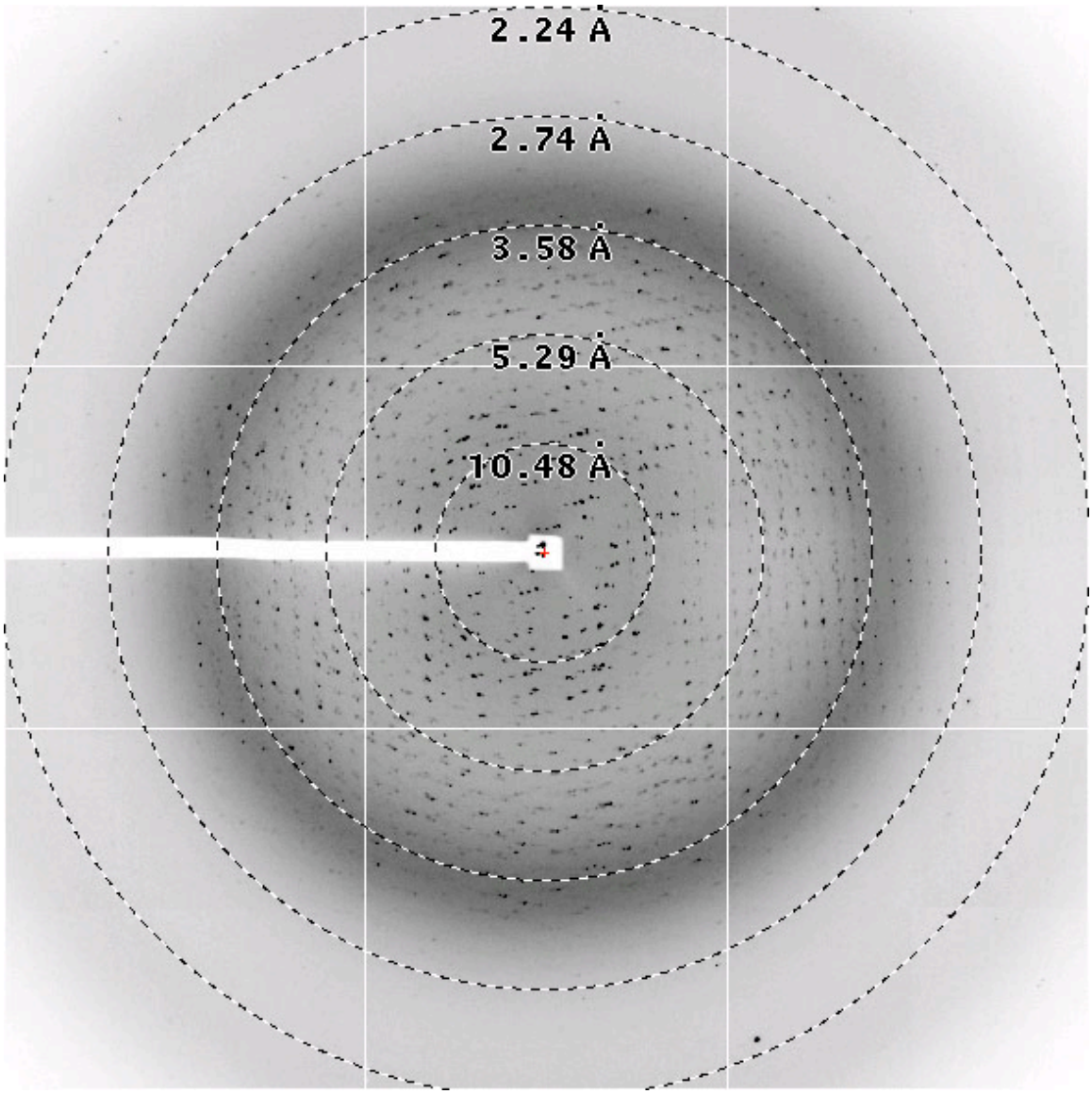

Figure A.4 Initial Diffraction Pattern of McpB
Overlap of diffraction pattern of multiple crystals rendered the data useable because the unit cell could not be determined. Even with the unit cell the spots overlap so much that integration would not be successful.

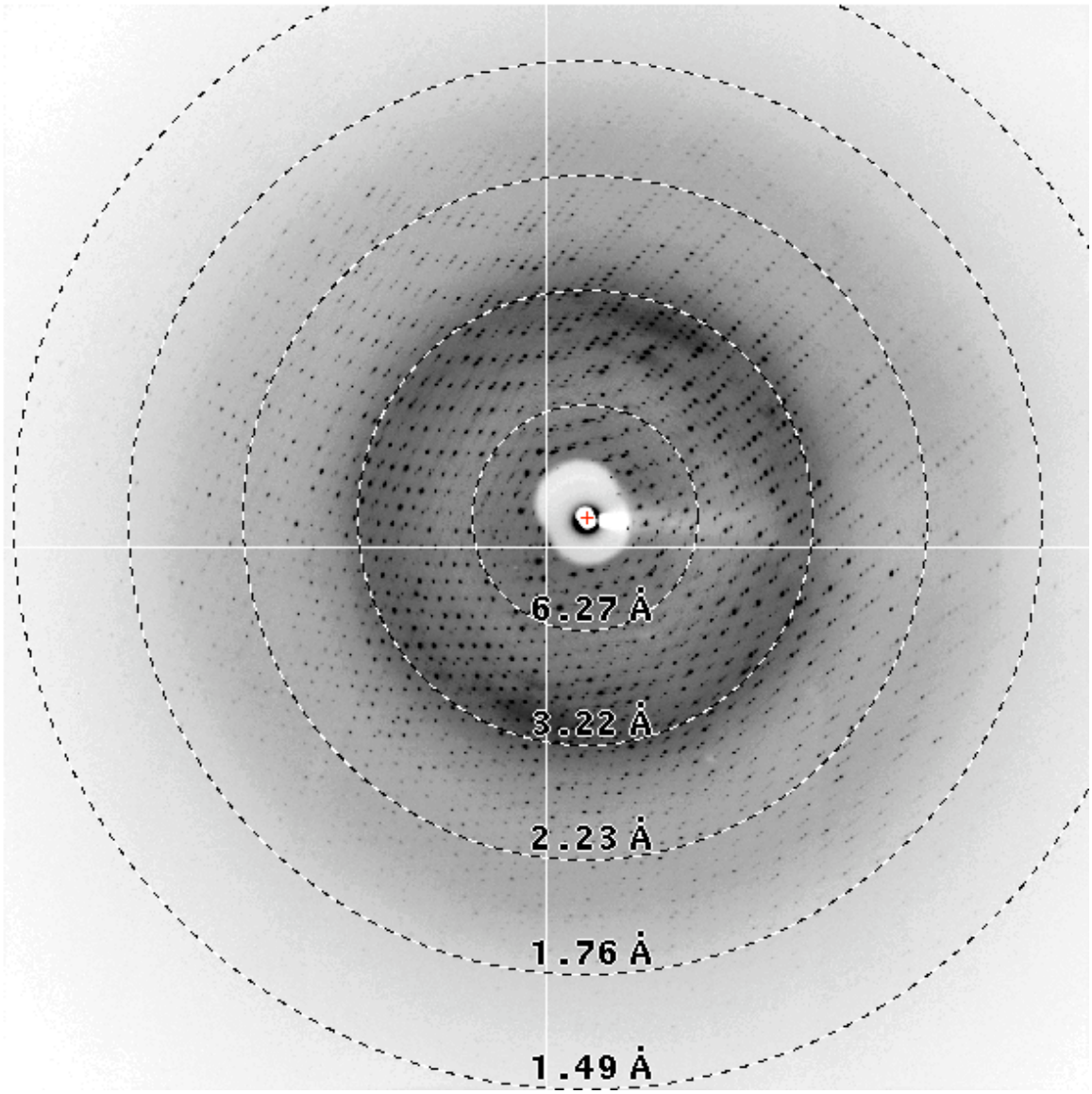

Figure A.5 Improved McpB diffraction pattern using sodium malonate as an additive.
There is still a bit of overlap with another crystal lattice particularly in the low resolution range. However one lattice dominates and the data was easily indexed by HKL2000. The spots look relatively clean however the data is twinned in all three dimensions.

Determination of the space group for McpB was not straightforward because of pseudo-symmetry and twinning. Initially some data sets indexed and scaled well as centered orthorhombic but these crystals seem to have a higher twinning fraction. The twinning operation because it is along the diagonal between a and c is mimicking another two-fold.

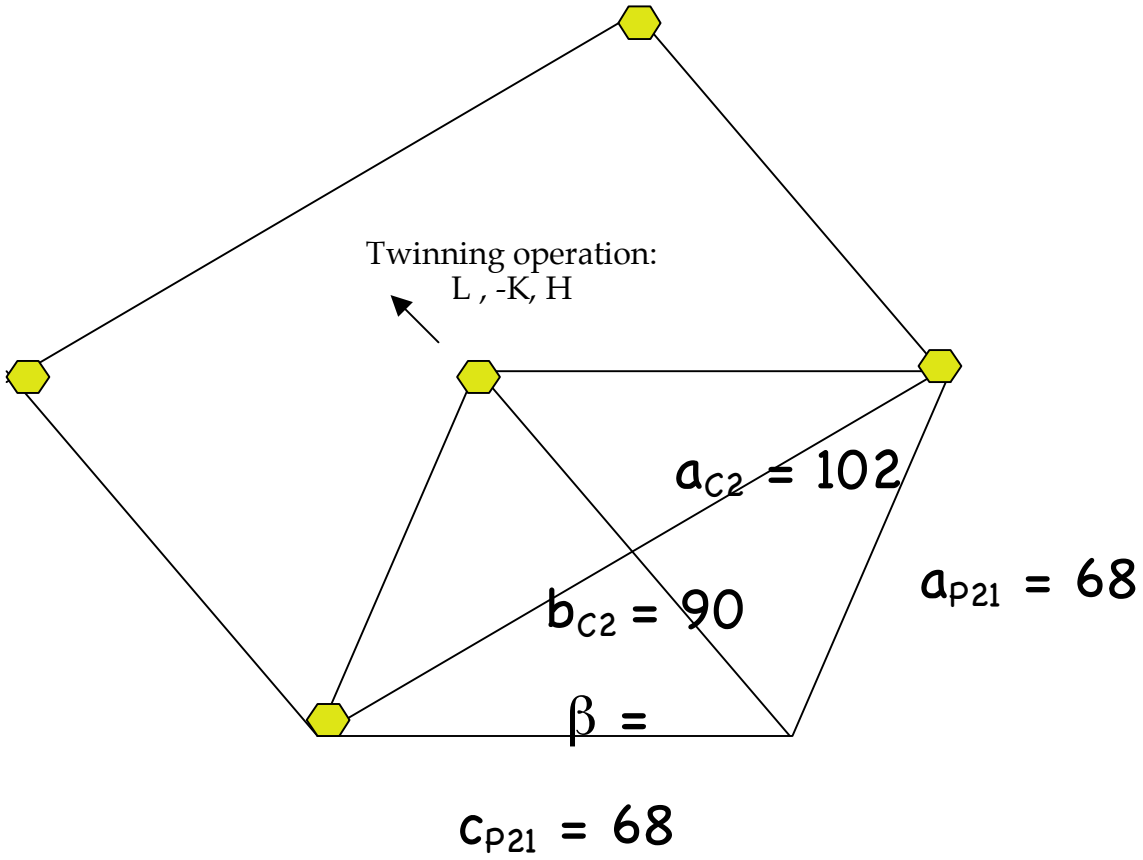

Figure A.6 Representation of the relationship between the potential symmetry group for McpB and twinning operation. The parallelogram is the formed by a = 68 and c = 68. The beta angle between the two axes is 97 degrees. The true two-fold of the monoclinic cell ($P2_1$) along b = 102 points out of the page. The yellow hexagrams trace out the centered monoclinic cell (C2). The twinning occurs along the diagonal between a and c thus the operation that relates the twinning is L, -K, H. This diagonal is the b = 90 of the C2 cell. With centered monoclinic the beta angle is very close to 90 degrees causing the symmetry to appear to be higher order (centered orthrorhombic: C222).

Table A.1 Data collected on 5 different crystals.

	SePe26	SePeX2	SePeak	SePe2	McpB
C2 $\beta \sim 90^o$	Rsym=40% a: 102 b: 90 c: 102	Rsym=42% a: 102 b: 90 c: 102	Rsym=18% a: 102 b: 90 c: 102	Rsym=22% a: 102 b: 90 c: 102	Rsym=12% a: 102 b: 90 c: 102
P21 $\beta \sim 97^o$	Rsym=10% a: 68 b: 102 c: 68	Rsym=10% a: 68 b: 102 c: 68	Rsym=15% a: 68 b: 102 c: 68	Rsym=10% a: 68 b: 102 c: 68	Rsym=10% a: 68 b: 102 c: 68
C222	Rsym=41% a: 90 b: 102 c: 102	Rsym=38% a: 90 b: 102 c: 102	Rsym=17% a: 90 b: 102 c: 102	Rsym=17% a: 90 b: 102 c: 102	Rsym=8% a: 90 b: 102 c: 102

This table shows the Rsym for 5 different crystals processed as three different symmetry groups. The ones with lowest Rsym in C222 were the most twinned as expected.

Table A.2 A table of some of the data sets collected for McpB.

Data set	Unit cell	β	Highest Resolution	Rsym in lowest resolution shell	Rsym in highest resolution shell	Overall Rsym	Completeness	Redundancy	2nd moment	Wilson B	H alpha	Britton alpha	Max. likelihood twinning fraction
output10.sca	68.48 102.14 68.53	97.3	1.7 Å	0.055	0.41	0.081	98.40%	3.3	1.85	21	0.329	0.353	0.217
SePe2.sca	68.63 103.29 68.61	97.42	2.3 Å	0.107	0.37	0.15	95.90%	7.2	1.71	32	n/a	n/a	n/a
outSePe2_7.sca	68.72 103.25 68.55	97.44	2.3 Å	0.078	0.2	0.099	96.90%	6.9	1.63	27	0.4	0.4	0.34
Se26.sca	68.39 101.90 68.29	97.3	2.6 Å	0.066	0.42	0.1	99.80%	6.9	1.87	44	0.14	0.13	0.04
outputx20p21.sca	68.39 102.67 68.67	97.34	2.3 Å	0.081	0.3	0.11	95.60%	3	2.06	33	0.12	0.09	0.07
G10output2.sca	68.86 102.56 68.50	97.86	3.30 Å	0.078	0.31	0.154	97.70%	3.5	1.99	39	0.16	0.21	0.07
A1_5.sca	68.78 100.91 68.55	97.59	3.0 Å	0.097	0.38	0.11	64.10%	1.9	2.46	57	0.08	0.03	0.02
pkI_output2.sca	68.56 104.18 68.80	97.41	2.4 Å	0.12	0.4	0.15	86.40%	1.7	2.11	35	0.12	0.14	0.09
all_I1I2_6.sca	68.93 104.45 68.66	97.49	2.4 Å	0.08	0.37	0.13	99.90%	11.3	2.08	33	0.046	0.03	0.022

The native data sets are in purple, the selenomethionine data sets are in blue, and the heavy atom data sets (Hg) are in green.

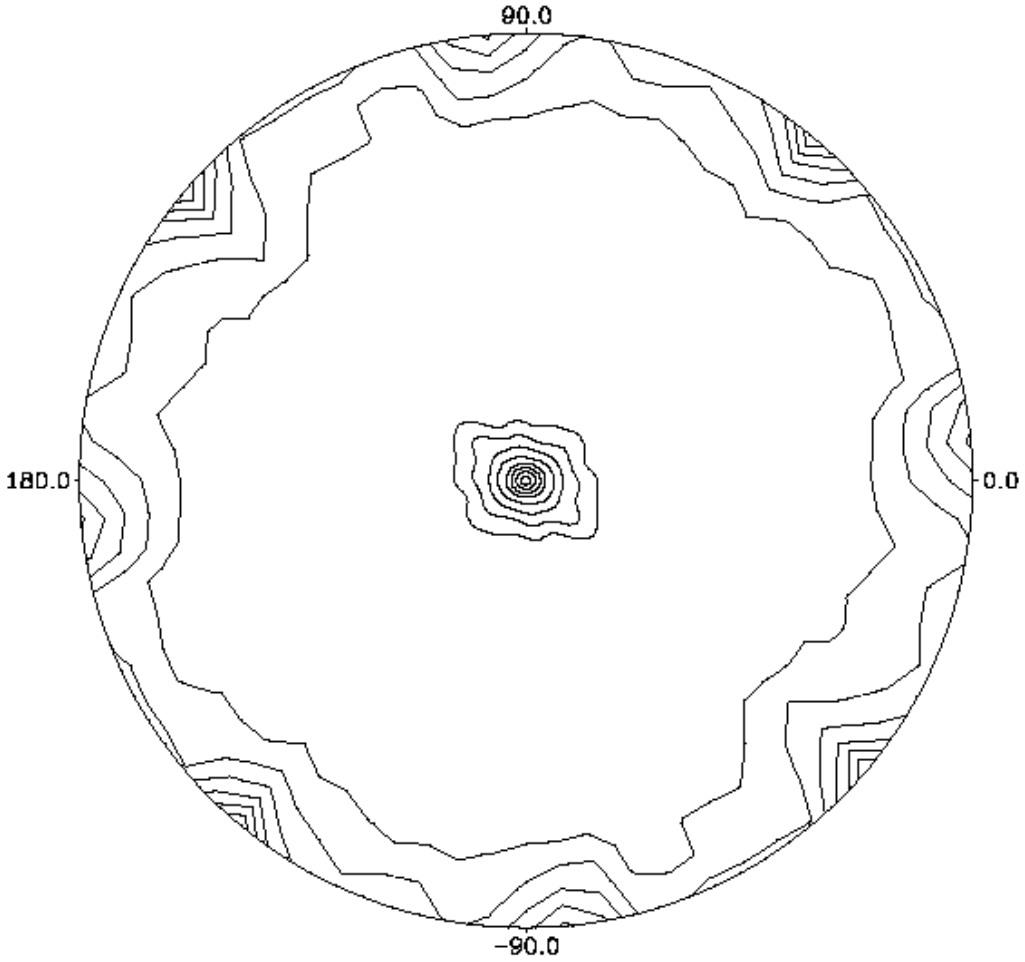

Figure A.7 Self-rotation function of output10.sca [McpB crystal] - the native data set. The twinning along the diagonal between a and c is seen through the peaks that occur in between the axes. The peaks that occur just off the axes are most likely due to non-crystallographic symmetry – a pseudo-two fold.

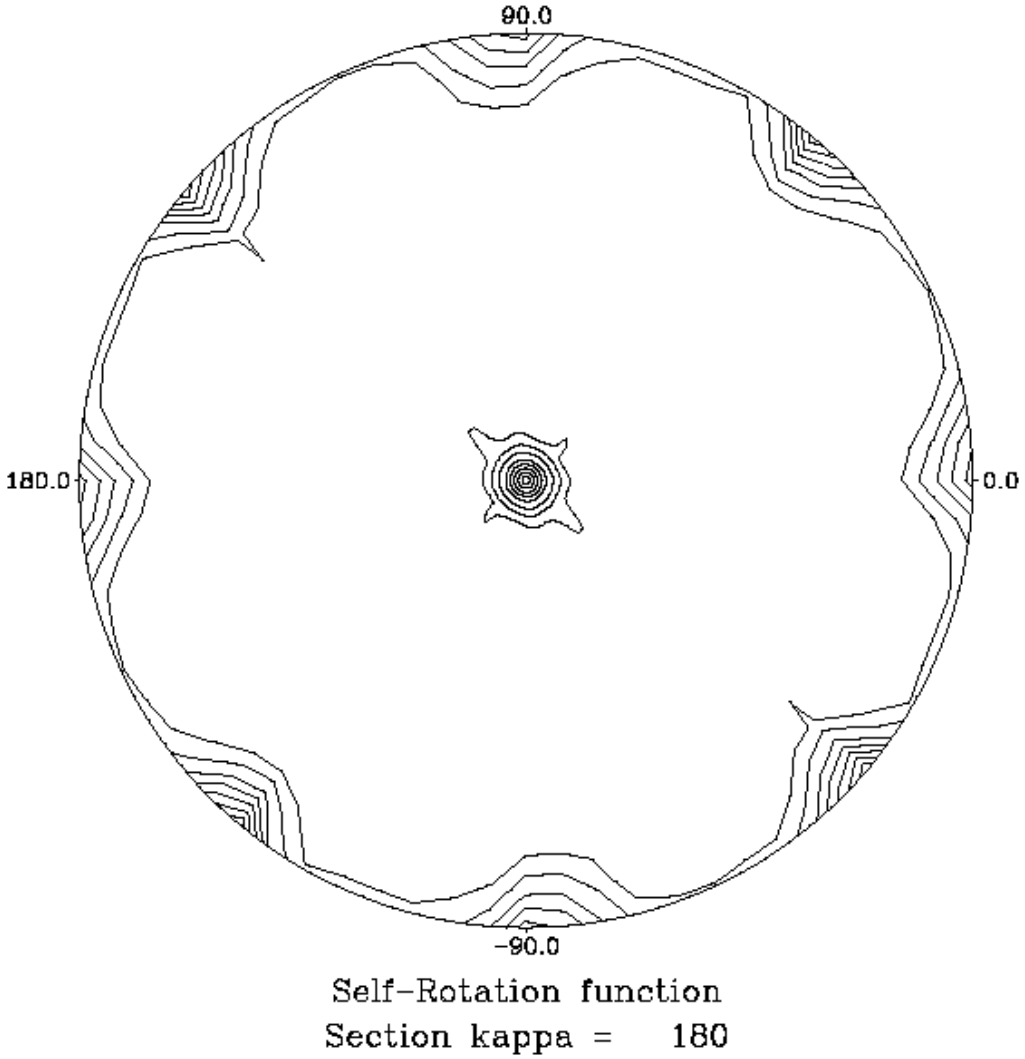

Figure A.8 Self-Rotation function of outSePe2_7.sca [SePe2 – crystal]
Strong peaks on the diagonal between a and c indicative of the high twinning fraction of this crystal.

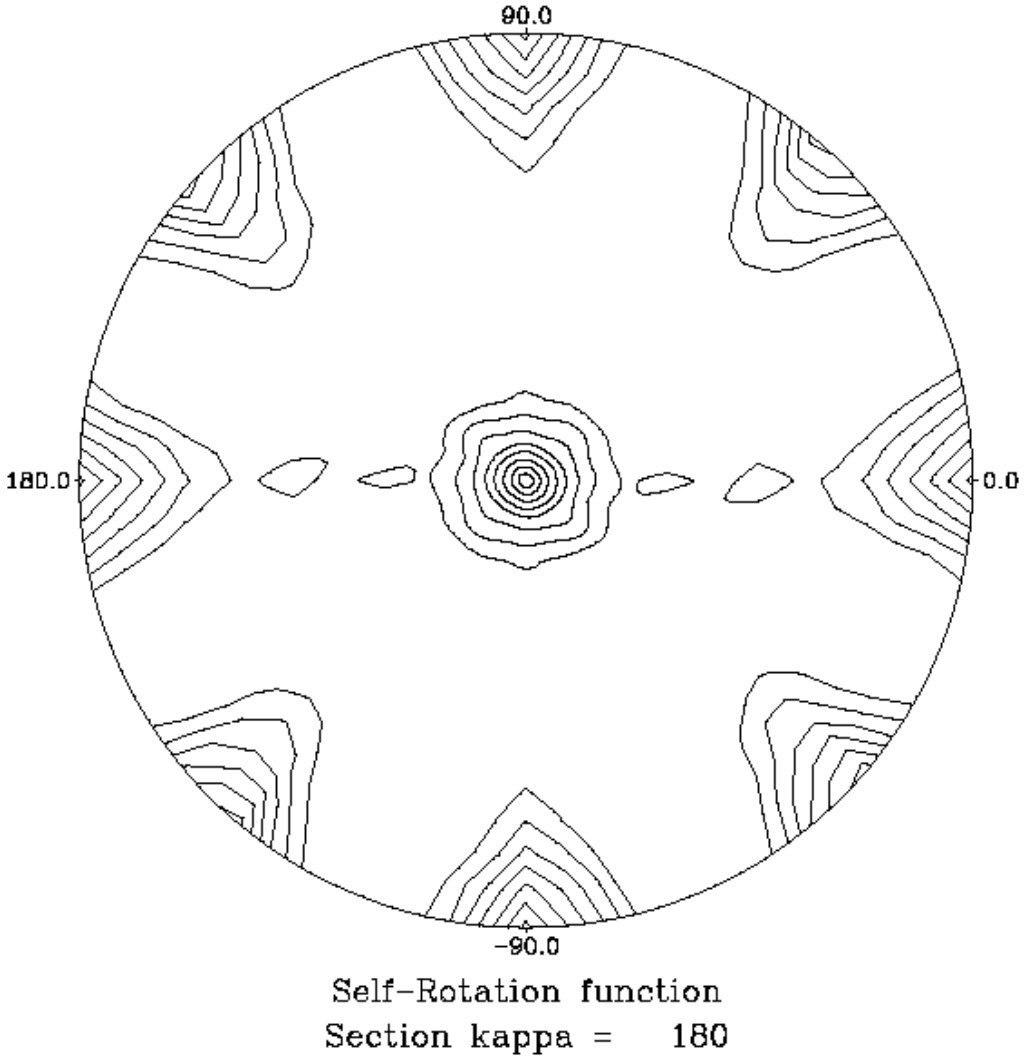

Figure A.9 Self-Rotation function of Se26.sca [SePe26 – crystal] – Surprisingly the twinning peaks are quite strong but the estimated twinning fraction for this crystal is lower than other crystals.

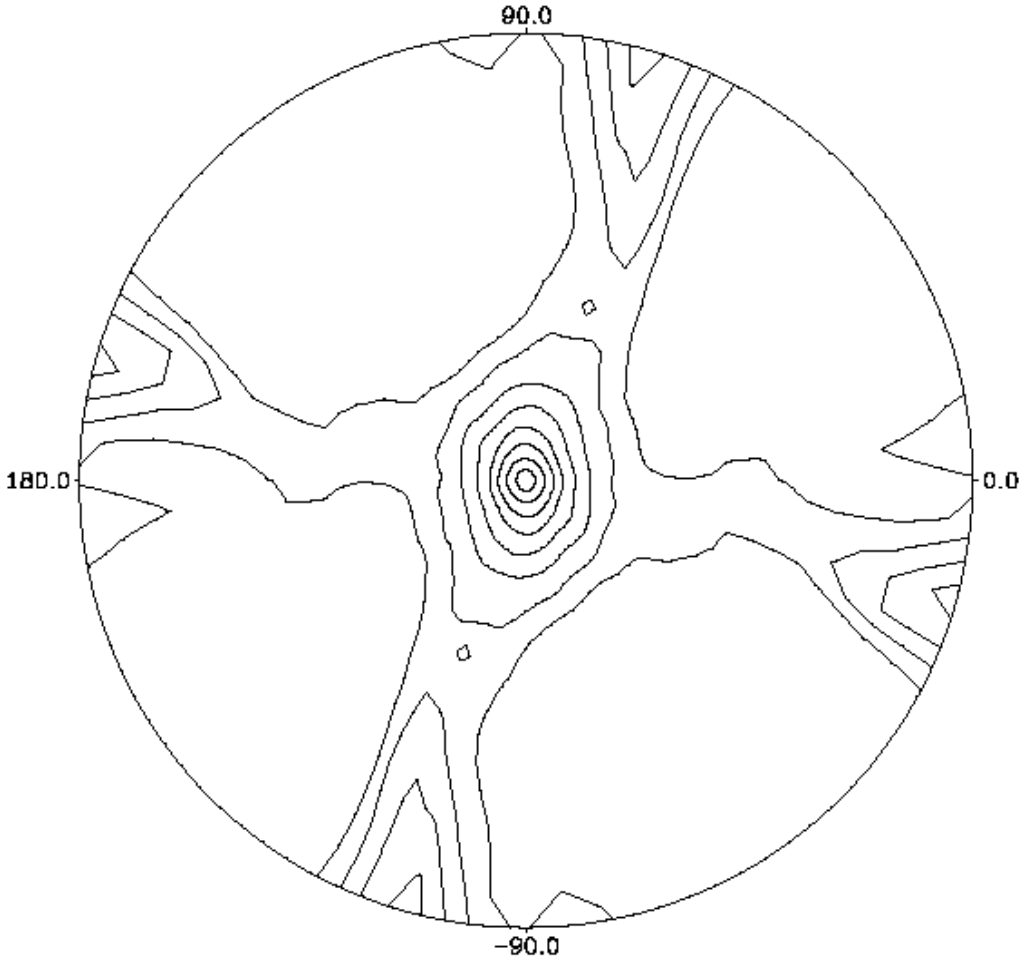

Figure A.10 Self-Rotation function of outputx20p21.sca [SePeX2 – crystal]
This crystal is the least twinned according to the lack of twinning peaks. However it would appear that the non-crystallographic symmetry is still present creating the peaks that are slightly off the axes.

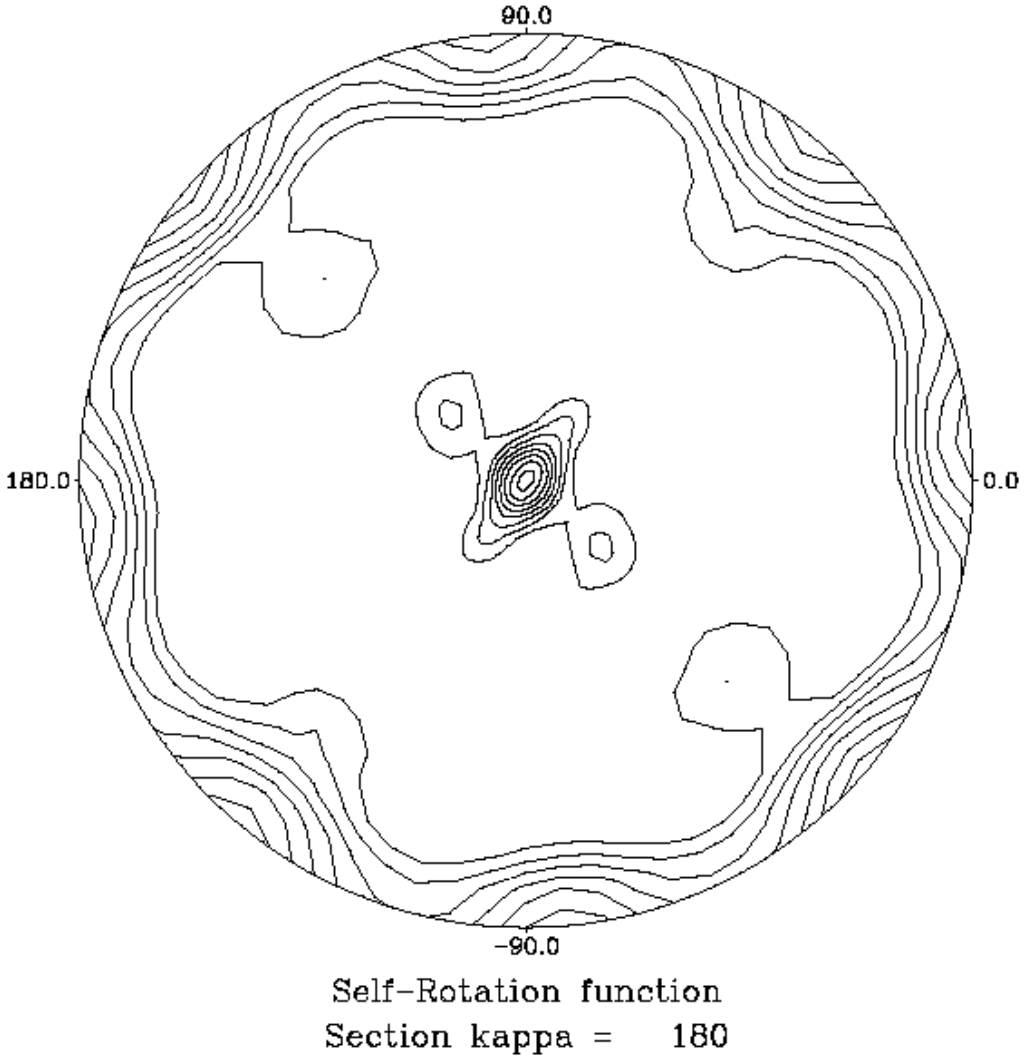

Figure A.11 Self-Rotation function of G10output2.sca [G10 crystal co crystallized with Hg].

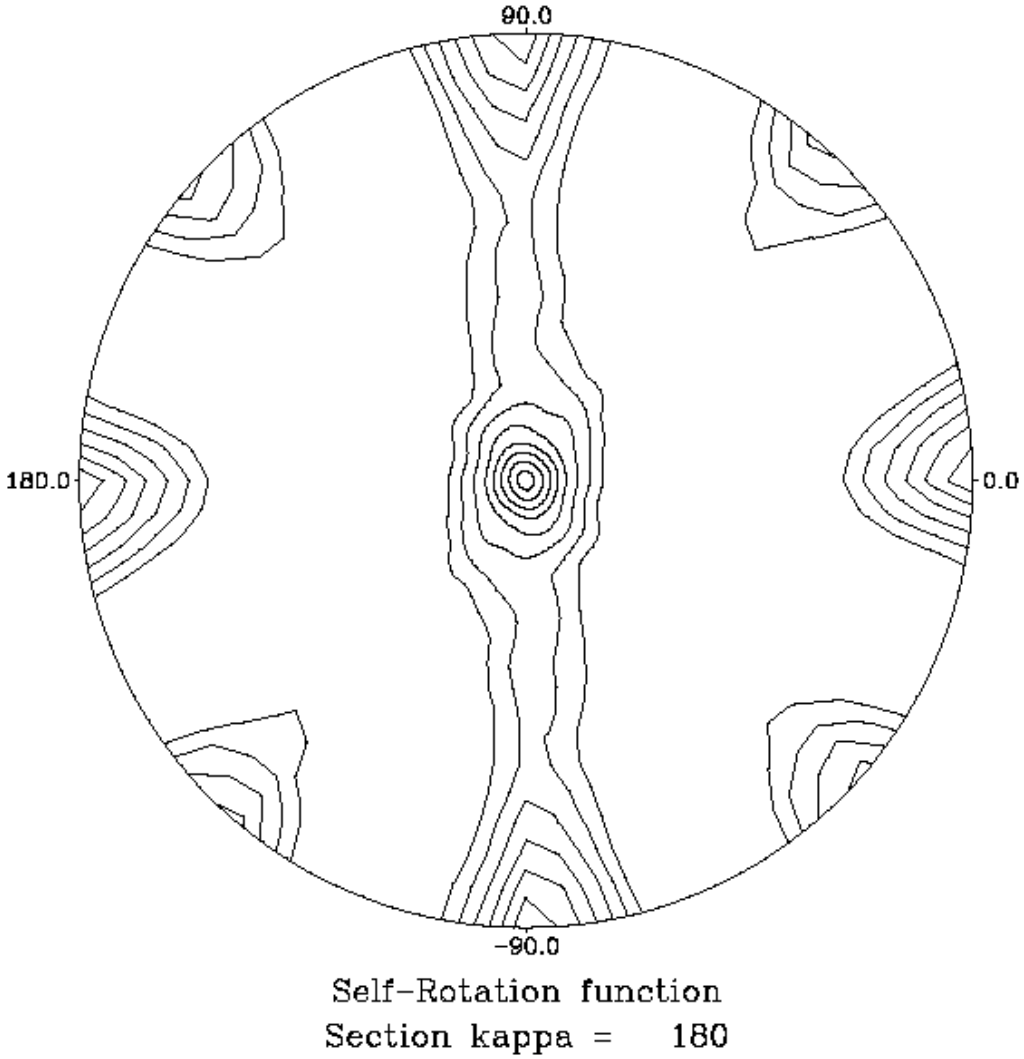

Figure A.12 Self-Rotation function of all_I1I2_6.sca [I1 crystal – co crystallized with Hg].
Twinning peaks lower than other structures also the estimated twinning fraction is low. Pseudo-symmetry however is high.

REFERENCES

(1) Falke, J. J., and Hazelbauer, G. L. (2001) Transmembrane signaling in bacterial chemoreceptors. *Trends Biochem. Sci. 26*, 257-265.

(2) Milburn, M. V., Prive, G. G., Milligan, D. L., Scott, W. G., Yeh, J., Jancarik, J., Koshland, D. E., and Kim, S. H. (1991) 3-Dimensional Structures Of The Ligand-Binding Domain Of The Bacterial Aspartate Receptor With And Without A Ligand. *Science 254*, 1342-1347.

(3) Danielson, M. A., Biemann, H. P., Koshland, D. E., and Falke, J. J. (1994) Attractant-Induced And Disulfide-Induced Conformational-Changes In The Ligand-Binding Domain Of The Chemotaxis Aspartate Receptor - A F-19 Nmr-Study. *Biochemistry 33*, 6100-6109.

(4) Chervitz, S. A., and Falke, J. J. (1995) Lock On Off Disulfides Identify The Transmembrane Signaling Helix Of The Aspartate Receptor. *Journal Of Biological Chemistry 270*, 24043-24053.

(5) Chervitz, S. A., Lin, C. M., and Falke, J. J. (1995) Transmembrane Signaling By The Aspartate Receptor - Engineered Disulfides Reveal Static Regions Of The Subunit Interface. *Biochemistry 34*, 9722-9733.

(6) Chervitz, S. A., and Falke, J. J. (1996) Molecular mechanism of transmembrane signaling by the aspartate receptor: a model. *Proc Natl Acad Sci U S A 93*, 2545-50.

(7) Anantharaman, V., and Aravind, L. (2000) Cache - a signaling domain common to animal Ca2+ channel subunits and a class of prokaryotic chemotaxis receptors. *Trends In Biochemical Sciences 25*, 535-537.

(8) Szurmant, H., Bunn, M. W., Cho, S. H., and Ordal, G. W. (2004) Ligand-induced conformational changes in the Bacillus subtilis chemoreceptor

McpB determined by disulfide crosslinking in vivo. *J Mol Biol 344*, 919-28.

(9) Sevvana, M., Vijayan, V., Zweckstetter, M., Reinelt, S., Madden, D. R., Herbst-Irmer, R., Sheldrick, G. M., Bott, M., Griesinger, C., and Becker, S. (2008) A ligand-induced switch in the periplasmic domain of sensor histidine kinase CitA. *Journal Of Molecular Biology 377*, 512-523.